ANTIOXIDANTS & REDOX SIGNALING
Volume 15, Number 6, 2011

DOI: 10.1089/ars.2010.3454

ORIGINAL RESEARCH COMMUNICATION

Central Apelin Controls Glucose Homeostasis *via* a Nitric Oxide-Dependent Pathway in Mice

Thibaut Duparc,[1,2] André Colom,[1,2] Patrice D. Cani,[3] Nicolas Massaly,[4] Sophie Rastrelli,[1,2] Anne Drougard,[1,2] Sophie Le Gonidec,[1] Lionel Moulédous,[5] Bernard Frances,[4] Isabelle Leclercq,[6] Catherine Llorens-Cortes,[7] J. Andrew Pospisilik,[8] Nathalie M. Delzenne,[3] Philippe Valet,[1,2] Isabelle Castan-Laurell,[1,2] and Claude Knauf[1,2]

Abstract

Aims: Apelin and its receptor have emerged as promising targets for the treatment of insulin resistance. Indeed, peripheral administration of apelin stimulates glucose utilization and insulin sensitivity via a nitric oxide (NO) pathway. In addition to being expressed on peripheral metabolically active adipose tissues, apelin is also found in the brain. However, no data are available on the role of central effects of apelin on metabolic control. We studied glucose metabolism in response to acute and chronic intracerebroventricular (i.c.v.) injection of apelin performed in normal and obese/diabetic mice. ***Results:*** We demonstrate that i.c.v. injection of apelin into fed mice improves glucose control via NO-dependent mechanisms. These results have been strengthened by transgenic (eNOS-KO mice), pharmacological (L-NMMA i.c.v. treated mice), and real-time measurement of NO release with amperometric probes detection. High-fat diet-fed mice displayed a severely blunted response to i.c.v. apelin associated with a lack of NO response by the hypothalamus. Moreover, central administration of high dose apelin in fasted normal mice provoked hyperinsulinemia, hyperglycemia, glucose intolerance, and insulin resistance. ***Conclusion:*** These data provide compelling evidence that central apelin participates in the regulation of glucose homeostasis and suggest a novel pathophysiological mechanism involved in the transition from normal to diabetic state. *Antioxid. Redox Signal.* 15, 1477–1496.

Introduction

EVERY YEAR THE NUMBER of described adipokines continues to grow (1). Their roles in physiological and physiopathological systems, including the development of metabolic syndrome, are well documented (28). Apelin is one of few adipokines whose expression pattern, and that of its cognate receptor (APJ), include peripheral tissue and central neurons (7, 11). During the last years, numerous studies have demonstrated a clear relation between energy metabolism and peripheral apelin action (12, 17, 19). Under normal conditions, a positive correlation is observed between plasma apelin and insulin levels during the fasting-to-fed transition (3, 18, 42). Under pathophysiological conditions, the peripheral apelinergic system seems to be deregulated. While some researchers found that

Innovation

Although apelin is expressed in hypothalamic neurons, nothing is known concerning its central effect in the control of glucose homeostasis. We demonstrate that apelin can modify hypothalamic neuron activity via an NO pathway and then control peripheral glycemia. Our results clearly show that central apelin has dose-dependent and pleiotropic effects depending on the nutritional state. Despite its beneficial effect observed at a low-dose level on glucose homeostasis, we suggest that a high dose of central apelin could be considered as a novel candidate for the transition from normal to diabetic state.

[1]Institut National de la Santé et de la Recherche Médicale (INSERM), U1048, Team 3, Toulouse, France.
[2]Université Paul Sabatier, UPS, Institut des Maladies Métaboliques et Cardiovasculaires (I2MC), CHU Rangueil, Toulouse Cedex 4, France.
[3]Louvain Drug Research Institute, LDRI, Metabolism and Nutrition Research Group, and [6]Laboratory of Hepato-gastroenterology, Institut de Recherche Experimentale et Clinique, Université Catholique de Louvain, Brussels, Belgium.
[4]Centre de Recherches sur la Cognition Animale, Université de Toulouse, Toulouse, France.
[5]Unité Mécanismes D'action des Substances Opioïdes, Institut de Pharmacologie et de Biologie Structurale, Centre National de la Recherche Scientifique Toulouse Cedex 04, France.
[7]INSERM U691, Collège de France, Paris, France.
[8]Max Planck Institute for Immunobiology, Freiburg, Germany.

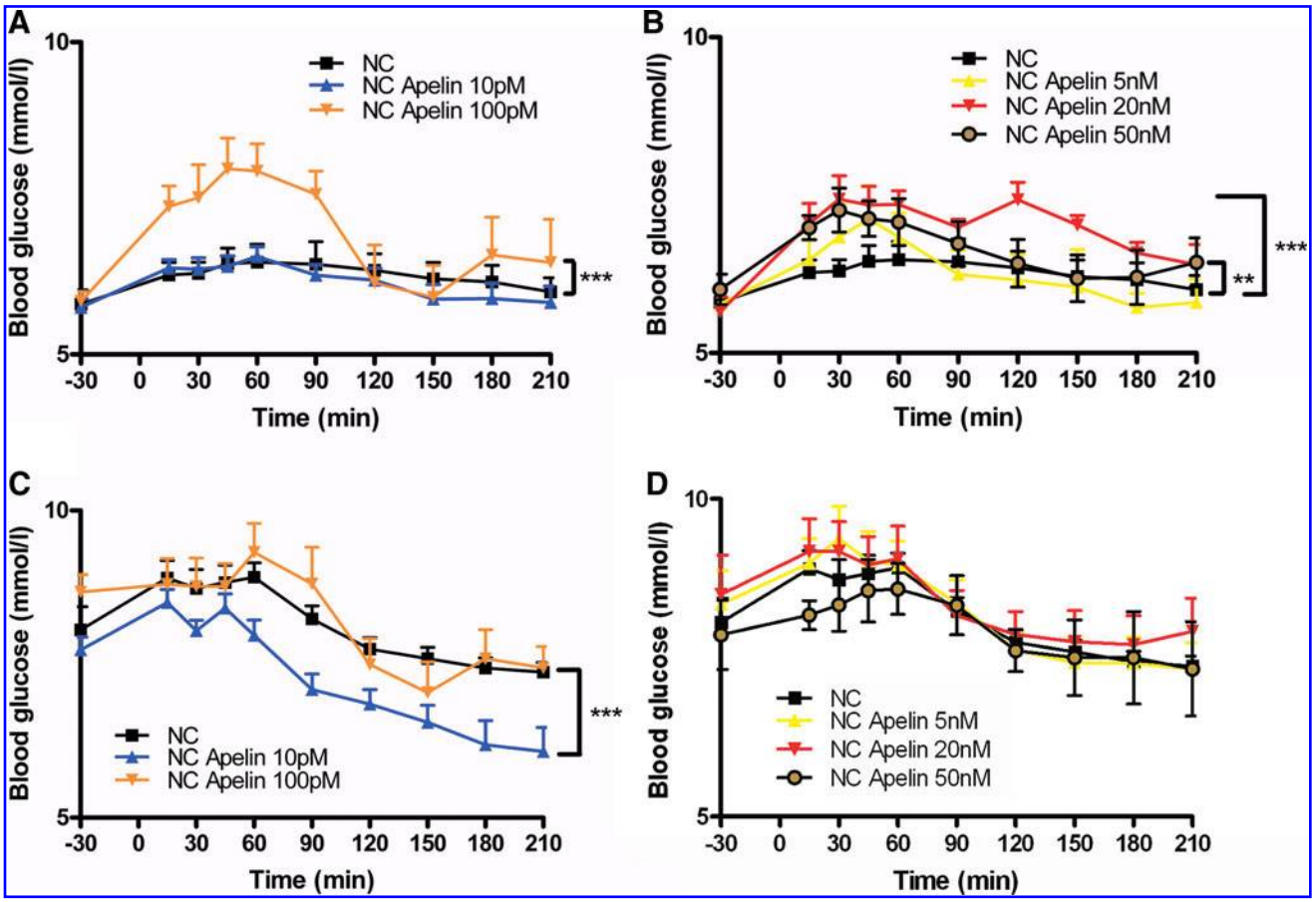

FIG. 1. Dose response of acute i.c.v. apelin injection on peripheral glycemia in fasted and fed state. **(A)** Effects of 10 p*M* and 100 p*M* apelin i.c.v. injected ($n=17$ and 6, respectively) on blood glucose in fasted normal chow (NC) WT mice compared to aCSF injected fasted NC WT mice (NC; $n=18$); ***$p<0.001$, NC vs. NC apelin 100 p*M* following one-way ANOVA analysis followed by Dunnett's *post-hoc* test. **(B)** Effects of 5 n*M*, 20 n*M*, and 50 n*M* apelin i.c.v. injected ($n=6$, 6, and 8, respectively) on blood glucose in fasted NC WT mice compared to aCSF injected fasted NC WT mice ($n=8$); **$p<0.01$, NC vs. NC apelin 50 n*M* and ***$p<0.001$, NC vs. NC apelin 20 n*M* following one-way ANOVA analysis followed by Dunnett's *post-hoc* test. **(C)** Effects of 10 p*M* and 100 p*M* apelin i.c.v. injected ($n=15$ and 8, respectively) on blood glucose in fed NC WT mice compared to aCSF injected fed NC WT mice ($n=10$). ***$p<0.001$, NC vs. NC apelin 10 p*M* following one-way ANOVA analysis followed by Dunnett's *post-hoc* test. **(D)** Effects of 5 n*M*, 20 n*M*, and 50 n*M* apelin i.c.v. injected (NC; n = 10, 8, and 6, respectively) on blood glucose in fed WT mice compared to aCSF injected fed WT mice (NC; $n=8$). Results are the mean ± SEM.

levels of plasma apelin in human and mice are increased in obesity, diabetes (18, 42), and in insulin resistance (12), other studies demonstrate that plasma apelin is reduced in type 2 diabetes patients (14). Recently, we have demonstrated that acute intravenous (iv) apelin decreases glycemia and increases glucose utilization in the whole body of mice fed normal chow (NC) by stimulating glucose uptake, especially in skeletal muscles via an AMPK and endothelial nitric oxide synthase (eNOS) dependent pathway (12). Also, in high-fat diet (HFD) induction of insulin-resistant mice; apelin improves glucose

FIG. 2. Brain low-dose (LD) apelin controls glucose homeostasis in NC wild-type (WT) mice. (A) Effect of acute i.c.v. injection of LD apelin ($n=17$) on blood glucose in fasted NC WT mice compared to aCSF injected fasted NC WT mice ($n=18$). The *adjacent bar graph* represents the average area under the curve (AUC). **(B)** Time course insulinemia evolution before and after i.c.v. injection of LD apelin (*black*, $n=5$) or aCSF (*white*, $n=5$) in another set of fasted NC WT mice. **(C)** Effect of i.c.v. injected LD apelin on blood glucose ($n=15$) in fed NC WT mice compared to aCSF injected fed NC WT mice ($n=15$). The *adjacent bar graph* represents the average AUC. *$p<0.05$. **(D)** Time course insulinemia evolution before and after i.c.v. injection of LD apelin (*black*, $n=6$) or aCSF (*white*, $n=5$) in another set of fed NC WT mice. **(E)** OGTT in 6-hour-fasted NC WT mice i.c.v. injected with LD apelin ($n=10$) or aCSF ($n=11$). The *adjacent bar graph* represents the average AUC; *$p<0.05$. Two-way ANOVA followed by *t*-test *post hoc* reveals time ($^{\#}p<0.001$) and treatment ($^{\S}p<0.001$) effects. **(F)** OGTT-associated insulinemia in 6-hour-fasted NC WT mice i.c.v. injected with LD apelin (*black*, $n=10$) or aCSF (*white*, $n=11$). **(G)** ITT in 6-hour-fasted NC WT mice i.c.v. injected with LD apelin ($n=9$) or aCSF ($n=12$); *$p<0.05$, **$p<0.01$. Two-way ANOVA followed by *t*-test *post hoc* reveals time ($^{\#}p<0.001$) and treatment ($^{\$}p<0.01$) effects. **(H)** Turnover (TO), hepatic glucose production (HGP), glucose infusion rate (GIR), glycolysis (Glycol), and glycogen synthesis (Gln Synth) obtained during an euglycemic hyperinsulinemic clamp in 6-hour-fasted NC WT mice i.c.v. injected with LD apelin ($n=6$) or aCSF ($n=5$). Results are the mean ± SEM.

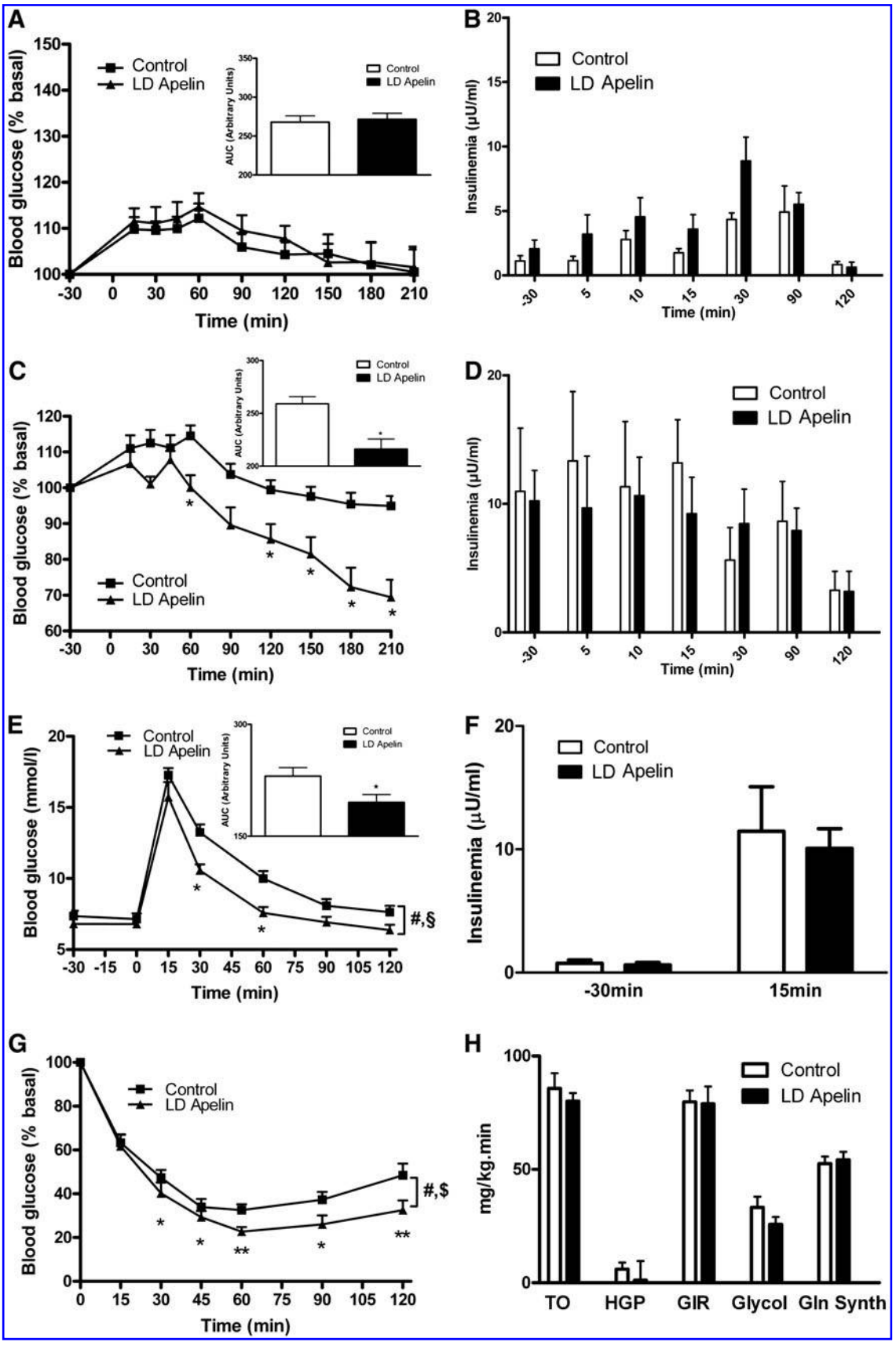
A
Blood glucose (% basal)
Control
LD Apelin
AUC (Arbitrary Units)
Time (min)
B
Insulinemia (µU/ml)
Control
LD Apelin
Time (min)
C
Blood glucose (% basal)
AUC (Arbitrary Units)
Control
LD Apelin
Time (min)
D
Insulinemia (µU/ml)
Control
LD Apelin
Time (min)
E
Blood glucose (mmol/l)
AUC (Arbitrary Units)
Control
LD Apelin
#,§
Time (min)
F
Insulinemia (µU/ml)
Control
LD Apelin
-30min
15min
G
Blood glucose (% basal)
Control
LD Apelin
#,$
Time (min)
H
mg/kg.min
Control
LD Apelin
TO
HGP
GIR
Glycol
Gln Synth

tolerance and insulin sensitivity (12), suggesting a potential compensatory role of the high levels of apelin observed in obese subjects. In keeping with these data, apelin KO mice are hyperinsulinemic and insulin resistant (49). Altogether, these data support a role for apelin in the control of glucose homeostasis.

The receptor APJ is expressed in several hypothalamic structures (10, 32, 33), including major targets of hormonal, nervous, and metabolic signals (22) that can modify hypothalamic activity. Apelinergic neuronal cell bodies are located in the preoptic region, the hypothalamic supraoptic and paraventricular nuclei, and at highest density in the arcuate nucleus (33). Apelinergic nerve fibers are also found in hypothalamic structures including the ventromedial and dorsomedial hypothalamic nuclei (VMH, DM), arcuate nucleus (ARC), and median eminence (33). Interestingly, intracerebroventricular (i.c.v.) insulin injection has been shown to modify two major peripheral apelin signaling mediators, AMPK (31) and eNOS (5), leading to an increase in peripheral glucose utilization. Although the localization of apelinergic neurons is well documented, the role of brain apelin/APJ system on glucose metabolism remains unknown.

The objective of this study was to investigate the role of brain apelin in the control of whole body glucose homeostasis. Using acute i.c.v. injection, we show that central apelin controls peripheral glycemia, insulin secretion, and glucose and insulin tolerance in mice. Using amperometric nitric oxide (NO) real-time measurement in the hypothalamus, pharmacological and transgenic approaches, we demonstrate that the beneficial effects of i.c.v. apelin are mediated through a NO-dependent signaling pathway that is altered in both HFD obese/diabetic mice and after administration of an acute high dose of i.c.v. apelin. In accordance with these data, we show that chronic i.c.v. perfusion of a high dose of apelin triggers the onset of metabolic alterations associated with type 2 diabetes, including a decrease in insulin tolerance. Thus, our data provide novel insight into the role of apelin in the central regulation of glucose homeostasis, and identify apelin as a novel central factor mediating the transition from a normal to insulin resistant state at high levels.

Results

Dose-response effect on glycemia in response to i.c.v. apelin in fasted or fed mice

Several hormones, such as the incretin glucagon-like peptide 1, exert their action only in hyperglycemic but not in euglycemic conditions (4). Based on this physiological finding, we speculate that apelin may exert an effect depending of the nutritional state. In accordance with this hypothesis, we found that high-dose of i.c.v. apelin increased glycemia in the fasted state (Figs. 1A and 1B) but not in the fed state (Figs. 1C and 1D). At the opposite, low-dose of i.c.v. apelin had no effect on fasted state (Fig. 1A), but decreased glycemia in fed conditions (Fig. 1C). Two doses (2 μl of 10 p*M* corresponding to 20.10^{-3} fmol, or 2 μl of 20 n*M* corresponding to 40 fmol) were selected for this study in respect to their effects on glycemia (Fig. 1). The first one (called "low-dose (LD)" in the text) was selected for its effect on fed glycemia, whereas the second one (called "high-dose (HD)") for its fasted hyperglycemic effect. The high dose (HD) of apelin (2 μl of 20 n*M*) corresponds approximately to half the quantity of total tissue apelin found in C57bl6 mouse hypothalamus (74 ± 4 fmoles per hypothalamus). These doses of apelin-13 injected iv did not modify blood glucose or insulin concentration (unpublished personal data).

Effect of acute i.c.v. LD apelin injection on peripheral glucose metabolism in physiological and pathophysiological conditions

In the fasted state, i.c.v. LD apelin injection did not significantly affect glycemia (Fig. 2A) and insulinemia (Fig. 2B). In the fed state, i.c.v. LD apelin induced a significant decrease in glycemia from 60 to 210 min (Fig. 2C), without altering insulin profiles (Fig. 2D). Further, LD apelin treatment significantly improved glucose tolerance in response to an oral glucose bolus (Fig. 2E). In keeping with the measures made during the fed state, insulin levels remained unchanged (Fig. 2F). Then, we performed an insulin tolerance test (ITT) at supraphysiological insulin dose (1 mU/g) and found that i.c.v. LD apelin-treated mice were more insulin tolerant compared to control (Fig. 2G). Nevertheless, euglycemic hyperinsulinemic clamp studies performed at physiological insulin levels (2.5 mU/kg/min) did not show any modification of the peripheral insulin sensitivity. Indeed, no modification of glucose turnover, hepatic glucose production, glucose infusion rate, glycolysis and glycogen synthesis (Fig. 2H) were observed in i.c.v. LD apelin-treated mice.

Given that during obese/diabetic states, resistance to central regulators of metabolism is often observed (30), we perfused i.c.v. LD apelin in HFD obese/diabetic mice. In the fasted state, i.c.v. LD apelin injection did not modify glycemia (Fig. 3A) and insulinemia (Fig. 3B). The potential improvement of glucose homeostasis of i.c.v. LD apelin was completely abolished in HFD conditions. Indeed, fed glycemia (Fig. 3C) and insulinemia (Fig. 3D), glucose tolerance (Figs. 3E and 3F) and insulin tolerance (Fig. 3G) of HFD i.c.v. treated LD apelin mice were similar to HFD control mice.

Circadian variations of plasma apelin levels in NC and HFD mice

We observed that i.c.v. LD apelin failed to improve glucose homeostasis parameters in HFD mice. One explanation for this result could be that hypothalamus, a circumven-

FIG. 3. Loss of beneficial effects on glucose homeostasis of acute i.c.v. LD apelin in HFD mice. (A) Effect of acute i.c.v. injection of LD apelin ($n = 10$) on blood glucose in fasted HFD WT mice compared to aCSF injected fasted HFD WT mice ($n = 9$). The *adjacent bar graph* represents the average AUC. **(B)** Time-course insulinemia evolution before and after i.c.v injection of LD apelin (*black*, $n = 7$) or aCSF (*white*, $n = 6$) in another set of fasted HFD WT mice. **(C)** Effect of acute i.c.v. injection of LD apelin ($n = 8$) on blood glucose in fed HFD WT mice compared to aCSF injected fed HFD WT fed ($n = 6$). The *adjacent bar graph* represents the average AUC. **(D)** Time course insulinemia evolution before and after acute i.c.v. injection of LD apelin (*black*, $n = 7$) or aCSF (*white*, $n = 6$) in another set of fed HFD WT mice. **(E)** OGTT in 6-hour-fasted HFD WT mice i.c.v. injected with LD apelin ($n = 9$) or aCSF ($n = 10$). The *adjacent bar graph* represents the average AUC. **(F)** OGTT-associated insulinemia in 6-hour-fasted HFD WT mice i.c.v. injected with LD apelin (*black*, $n = 9$) or aCSF (*white*, $n = 10$). **(G)** ITT in 6-hour-fasted HFD WT mice i.c.v. injected with LD apelin ($n = 7$) or aCSF ($n = 8$). Results are the mean ± SEM.

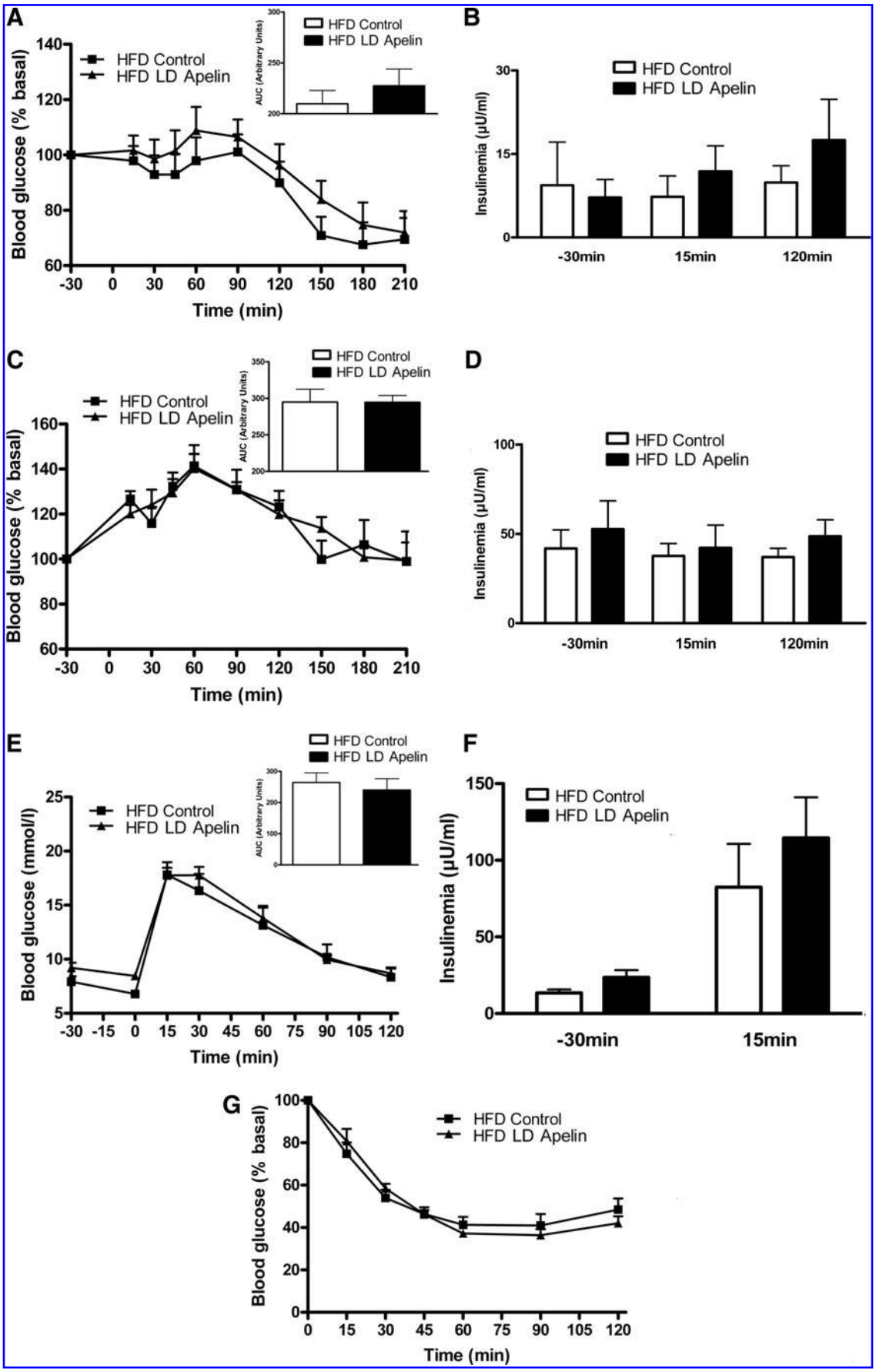
A
Blood glucose (% basal)
HFD Control
HFD LD Apelin
AUC (Arbitrary Units)
Time (min)
B
Insulinemia (µU/ml)
HFD Control
HFD LD Apelin
-30min
15min
120min
C
Blood glucose (% basal)
HFD Control
HFD LD Apelin
AUC (Arbitrary Units)
Time (min)
D
Insulinemia (µU/ml)
HFD Control
HFD LD Apelin
-30min
15min
120min
E
Blood glucose (mmol/l)
HFD Control
HFD LD Apelin
AUC (Arbitrary Units)
Time (min)
F
Insulinemia (µU/ml)
HFD Control
HFD LD Apelin
-30min
15min
G
Blood glucose (% basal)
HFD Control
HFD LD Apelin
Time (min)

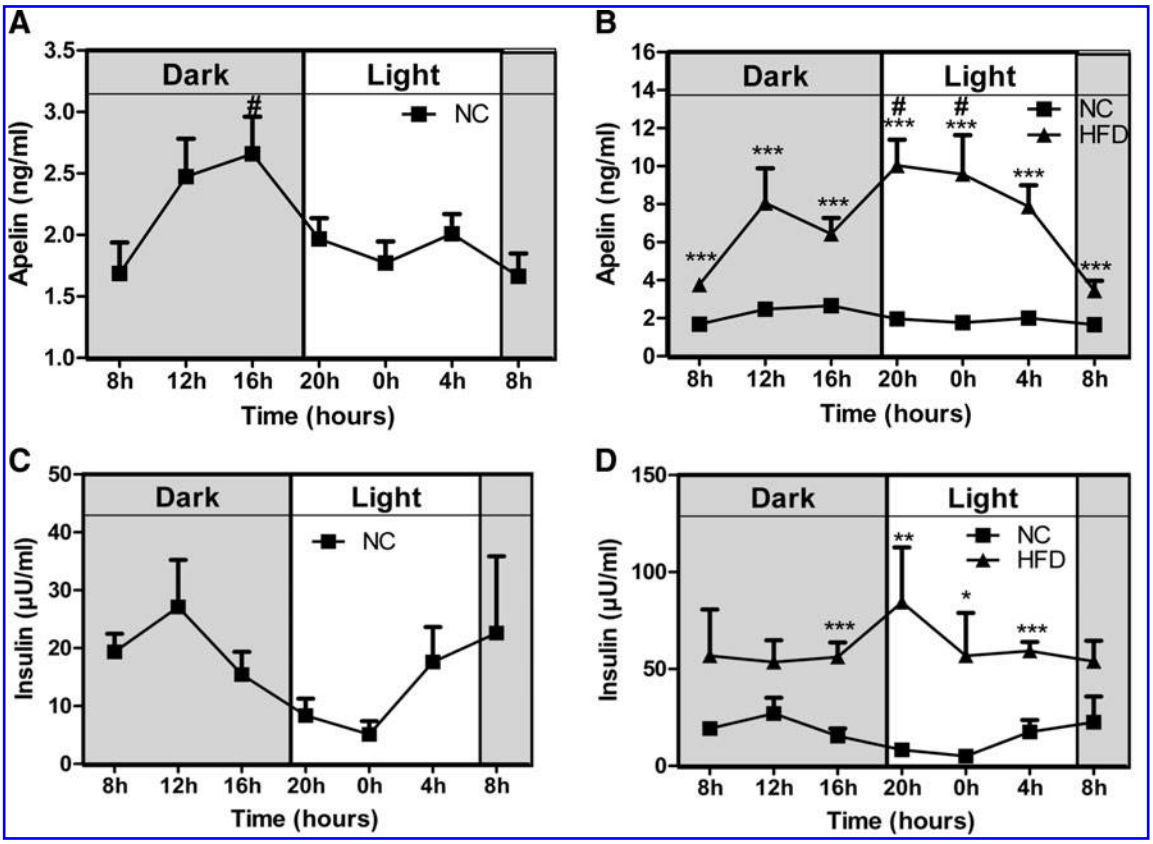

FIG. 4. Circadian plasma apelin variations are altered in HFD mice. (A) Circadian plasma apelin variations in NC WT mice ($n=5$). All data were compared to 8 hour. $^{\#}p<0.05$ vs. 8 hour following one-way ANOVA analysis followed by Dunnett's *post-hoc* test. **(B)** Circadian plasma apelin variations in HFD WT mice compared to NC WT mice ($n=5$). $^{***}p<0.001$ NC versus HFD; $^{\#}p<0.05$ vs. 8 hour following one-way ANOVA analysis, followed by Dunnett's *post-hoc* test. **(C)** Circadian plasma insulin variations in NC WT mice ($n=5$). **(D)** Circadian plasma insulin variations in HFD WT mice compared to NC WT mice ($n=5$); $^{*}p<0.05$, $^{**}p<0.01$, and $^{***}p<0.001$ NC versus HFD. Results are the mean ± SEM.

tricular structure where the blood–brain barrier displays physiological modifications (35), may be differentially stimulated by circulating apelin. In accordance with this hypothesis, we measured circadian variations of plasma apelin levels in physiological and physiopathological states. Plasma apelin levels in NC mice followed a circadian rhythm with an increase during the dark period (corresponding to the fed period) (Fig. 4A). In contrast to NC mice, HFD mice showed a deregulation of this rhythm since apelin plasma levels increased significantly during the entire day (Fig. 4B). As expected, plasma insulin levels follow a similar profile to those of apelin (Figs. 4C and 4D). This set of experiments supports the hypothesis that high levels of plasma apelin could contribute to brain neuronal alterations observed in obese/diabetic state.

Effect of acute i.c.v. of HD apelin injection on peripheral glucose metabolism in physiological and physiopathological conditions

As HFD mice showed altered circadian plasma apelin concentrations, we speculated that HD apelin could modify the physiological response of the brain. Acute i.c.v. HD apelin increased peripheral glycemia (Fig. 5A) and insulinemia (Fig.

FIG. 5. Acute i.c.v. injection of high-dose (HD) apelin alters glucose metabolism. (A) Effect of acute i.c.v. injection of HD apelin ($n=6$) on blood glucose in fasted NC WT mice compared to aCSF injected fasted NC WT mice ($n=18$). The *adjacent bar graph* represents the average AUC; $^{*}p<0.05$, $^{**}p<0.01$. **(B)** Time course insulinemia evolution before and after i.c.v. injection of HD apelin (*hatched*, $n=5$) or aCSF (*white*, $n=5$) in another set of fasted NC WT mice; $^{*}p<0.05$, $^{**}p<0.01$. **(C)** Effect of acute i.c.v. injection of HD apelin ($n=6$) on blood glucose in fed NC WT mice compared to aCSF injected fed NC WT mice ($n=8$). The *adjacent bar graph* represents the average AUC; $^{*}p<0.05$, $^{**}p<0.01$. **(D)** Time course insulinemia evolution before and after i.c.v. injection of HD apelin (*hatched*, $n=5$) or aCSF (*white*, $n=5$) in another set of fed NC WT mice; $^{*}p<0.05$, $^{**}p<0.01$. **(E)** OGTT in 6-hour-fasted NC WT mice i.c.v. injected with HD apelin ($n=7$) or aCSF ($n=11$). The *adjacent bar graph* represents the average AUC. **(F)** OGTT-associated insulinemia in 6-hour-fasted NC WT mice i.c.v. injected with HD apelin (*hatched*, $n=7$) or aCSF (*white*, $n=11$); $^{*}p<0.05$. **(G)** ITT in 6-hour-fasted NC WT mice i.c.v. injected with HD apelin ($n=12$) or aCSF ($n=12$). **(H)** Turnover (TO), hepatic glucose production (HGP), glucose infusion rate (GIR), glycolysis (Glycol), and glycogen synthesis (Gln Synth) obtained during an euglycemic hyperinsulinemic clamp in 6-hour-fasted NC WT mice i.c.v. injected with HD apelin ($n=6$) or aCSF ($n=5$); $^{*}p<0.05$, $^{**}p<0.01$. Results are the mean ± SEM.

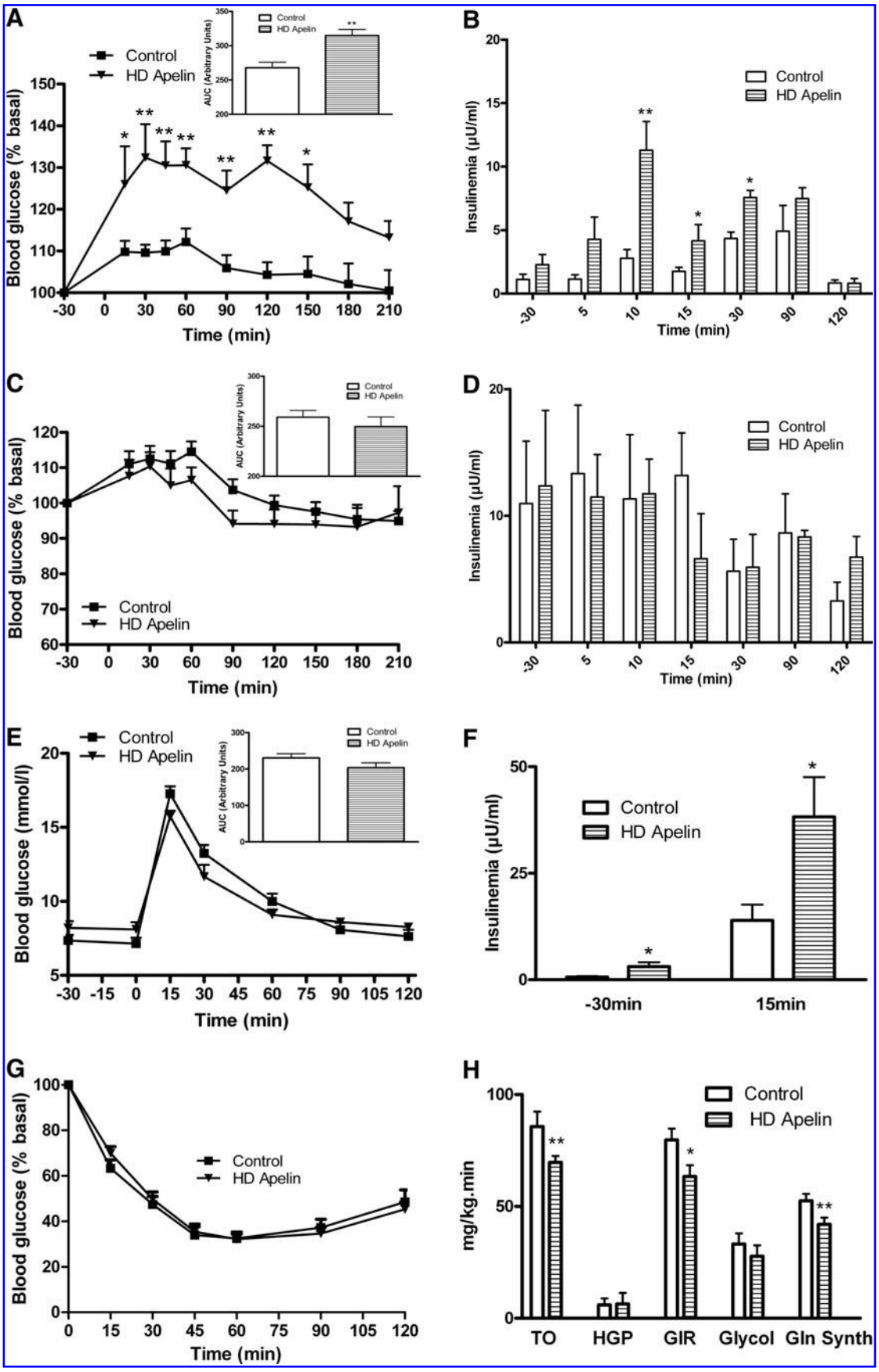
A
Control
HD Apelin
Blood glucose (% basal)
Time (min)
AUC (Arbitrary Units)
B
Insulinemia (µU/ml)
Time (min)
C
Blood glucose (% basal)
Time (min)
D
Insulinemia (µU/ml)
Time (min)
E
Blood glucose (mmol/l)
Time (min)
F
Insulinemia (µU/ml)
-30min
15min
G
Blood glucose (% basal)
Time (min)
H
mg/kg.min
TO
HGP
GIR
Glycol
Gln Synth

5B) in fasting normal mice. No significant variation of glycemia (Fig. 5C) and insulinemia (Fig. 5D) were observed in the fed state in response to i.c.v. HD apelin. Glucose tolerance was not modified in i.c.v. HD apelin treated mice compared to control (Fig. 5E), but was associated with a significant increase in insulinemia (Fig. 5F), suggesting a moderate insulin resistance state. Besides the fact that we did not observe any modification of the insulin tolerance upon supraphysiological insulin administration during ITT (Fig. 5G), euglycemic hyperinsulinemic clamp performed at physiological insulin dose confirmed that i.c.v. HD apelin promotes insulin resistance. Indeed, i.c.v. HD apelin decreased whole-body insulin sensitivity, as shown by the reduced glucose infusion rate and glucose turnover. This phenomenon was associated with a lower glycogen synthesis (Fig. 5H), whereas the other parameters were not affected. Because plasma apelin levels were increased during obesity and since we observed that injection of i.c.v. HD apelin induced hyperglycemia and hyperinsulinemia in NC mice, we investigated the effect of HD apelin i.c.v. injection in a HFD diabetic/obese mice model (12). In response to HD apelin, glycemia was significantly increased during fasting (Fig. 6A) without modification of insulinemia (Fig. 6B). Fed glycemia/insulinemia (Figs. 6C and 6D), glucose/insulin tolerance (Figs. 6E–6G) were not modified by acute i.c.v. HD apelin in HFD mice.

Variation of c-Fos expression in the hypothalamus in response to acute apelin injection in physiological conditions

Modifications of glycemia/insulinemia in response to acute i.c.v. apelin varied according to the injected dose and the nutritional state, raising the possibility that distinct hypothalamic regions were responsible for these effects. To test this hypothesis, we measured c-Fos expression in three major hypothalamic regions implicated in glucose metabolism under the previously tested conditions (22). I.c.v. bolus injection of LD apelin significantly increased c-Fos expression in the VMH and DM under fasting conditions, and only in the DM in the fed state in NC mice (Figs. 7A and 7B). c-Fos expression is significantly increased in the VMH and decreased in the ARC of HD apelin-treated mice in the fasted state (Fig. 7A). I.c.v. bolus injection of HD apelin did not modify c-Fos expression in studied hypothalamic regions (Fig. 7B). These data suggest that beneficial vs. deleterious effects of apelin may be explained by differential activation of hypothalamic regions. Thus, high quantity of apelin in the hypothalamus may be a crucial element to the establishment of a diabetic state.

Hypothalamic NO as a potential target to brain LD apelin

Given that hypothalamic NO is implicated in the control of glucose homeostasis (36) and NO is a major effector of apelin signaling in the periphery (12), we measured real-time NO release *ex vivo* in the hypothalamus in response to LD apelin. No significant variation on NO release was observed in hypothalamic slices removed from fasting animals (Fig. 8A). Delta variation of NO release from basal are similar to that observed previously (16). In fed state, LD apelin rapidly increased NO release from hypothalamic slices from 2 to 15 minutes (Fig. 8B). On hypothalamic explants, HD apelin did not increase NO release in fasting conditions (Fig. 8C), and failed to increase continuously NO release during the 20 minutes of the experiment in fed states as opposed to LD apelin (Fig. 8D). To explain such differences according to the nutritional state and apelin concentrations, we studied variations of eNOS expression on *ex vivo* hypothalamus stimulated by either LD or HD apelin. Contrary to HD apelin, which did not modify the ratio of phospho/total eNOS expression in all experimental conditions (Figs. 8E and 8F), LD apelin increased the active phosphorylated form of eNOS in fed (Fig. 8F) but not in fasted state (Fig. 8E). These results suggest that NO release from stimulated-LD apelin hypothalamus implicated an increase of eNOS activity. As we observed in HFD mice that 1) beneficial effect of LD apelin was impaired and, 2) hypothalamic eNOS pathway was seriously blunted in pathophysiological conditions (6), we studied the impact of LD or HD apelin on NO release from hypothalamic slices taken from HFD fed mice. No significant variation on NO release was observed in response to LD or HD apelin in fed state (Figs. 8G and 8H), and similar results were obtained in fasted conditions (data not shown).

Altogether these results suggest that obesity and insulin-resistant state participate to the disruption of the apelin-NO-dependent hypothalamic response.

Effect of acute i.c.v. LD or HD apelin on peripheral glucose metabolism in total eNOS KO and L-NMMA i.c.v. control treated mice

To address the dependence of the observed central apelin effects on the generation of NO, we repeated the above experiments in total eNOS KO mice. All beneficial effects of apelin on glucose homeostasis were lost in eNOS KO mice, including glucose tolerance (Figs. 9A and 9B) and fed glycemia (AUC: eNOS KO Control = 224.8 ± 14.9 vs. eNOS KO Apelin = 205.5 ± 12.3). eNOS KO mice perfused with i.c.v. NO donor did not present modification of glucose tolerance (ex-

FIG. 6. Persistent hyperglycemic effect of i.c.v. HD apelin on glucose homeostasis in HFD mice. (A) Effect of acute i.c.v. injection of HD apelin ($n = 6$) on blood glucose in fasted HFD WT mice compared to aCSF injected fasted HFD WT mice ($n = 5$). The *adjacent bar graph* represents the average AUC; $^{*}p < 0.05$, $^{**}p < 0.01$. **(B)** Time course insulinemia evolution before and after i.c.v. injection of HD apelin (*hatched*, $n = 6$) or aCSF (*white*, $n = 6$) in another set of fasted HFD WT mice. **(C)** Effect of acute i.c.v. injection of HD apelin ($n = 6$) on blood glucose in fed HFD WT mice compared to aCSF injected fed HFD WT mice ($n = 8$). The *adjacent bar graph* represents the average AUC. **(D)** Time course insulinemia evolution before and after i.c.v. injection of HD apelin (*hatched*, $n = 6$) or aCSF (*white*, $n = 6$) in another set of fasted HFD WT mice. **(E)** OGTT in 6-hour-fasted HFD WT mice i.c.v. injected with HD apelin ($n = 8$) or aCSF ($n = 10$). The *adjacent bar graph* represents the average AUC. **(F)** OGTT-associated insulinemia in 6-hour-fasted HFD WT mice i.c.v. injected with HD apelin (*hatched*, $n = 8$) or aCSF (*white*, $n = 10$). **(G)** ITT in 6-hour-fasted HFD WT mice i.c.v. injected with HD apelin ($n = 8$) or aCSF ($n = 8$). Results are the mean ± SEM.

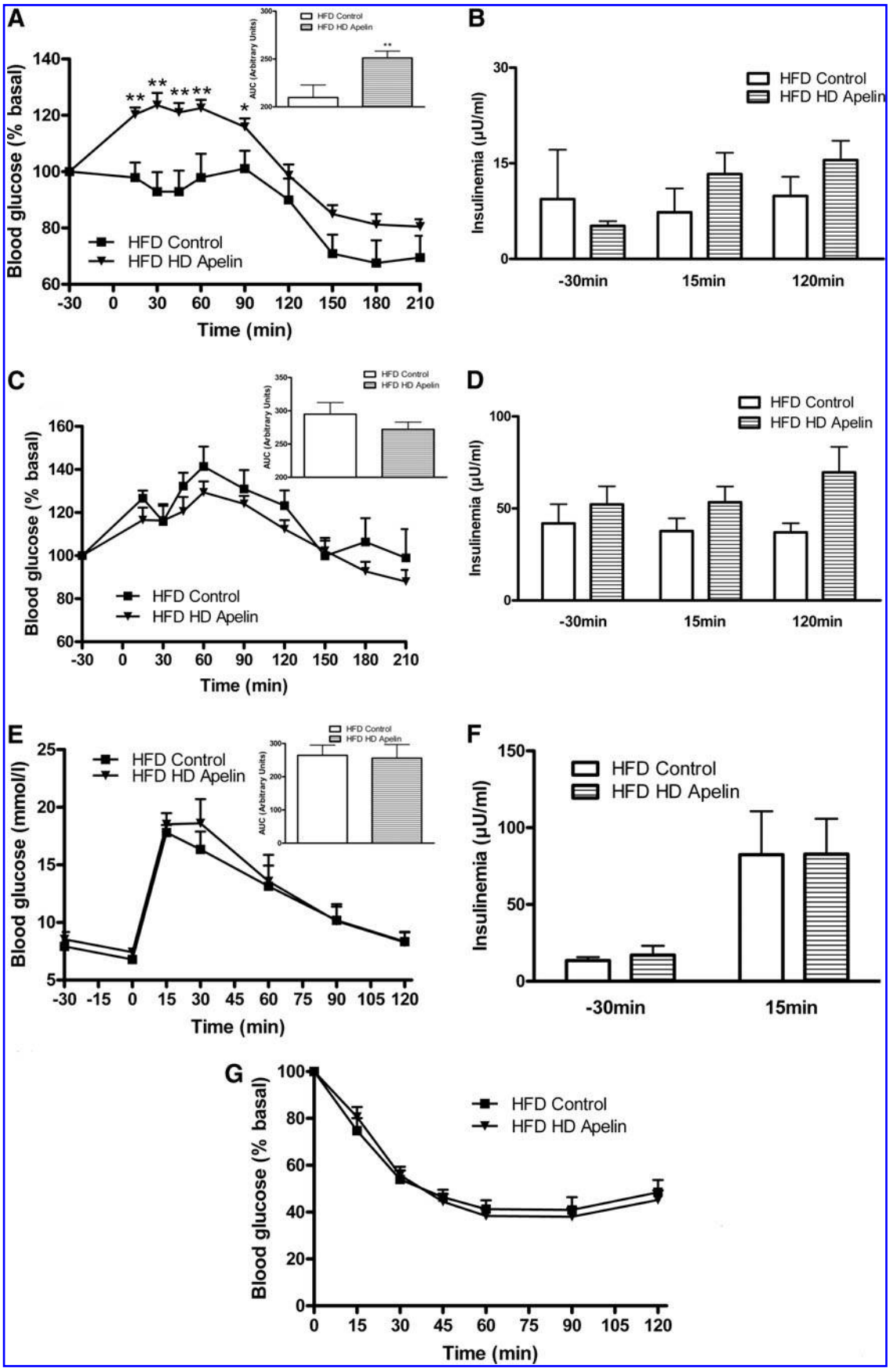
A
Blood glucose (% basal)
Time (min)
HFD Control
HFD HD Apelin
AUC (Arbitrary Units)
B
Insulinemia (µU/ml)
-30min
15min
120min
C
D
E
Blood glucose (mmol/l)
F
G

cept a slight decrease of glycemia at t60 and t90 following SNAP i.c.v. administration in eNOS KO mice) (Fig. 9A) associated with a drastic increase in insulin release (Fig. 9B). This suggests that 1) the lack of response to LD apelin could be at least in part due to the absence of a functional hypothalamic eNOS, and 2) insulin resistance is one major characteristic of eNOS KO mice (37). In accordance with these findings, pharmacological blockade of NOS using L-NMMA administration in wild-type mice completely abolished the beneficial effects of apelin observed on glucose homeostasis (Figs. 9C and 9D). Then we found that LD apelin did not increase NO release from *ex vivo* hypothalamus taken from eNOS KO mice (Fig. 9E) or from *ex vivo* control hypothalamus incubated with L-NMMA (Fig. 9F).

As we observed that beneficial effect of LD apelin on fed glycemia in NC mice requires a functional hypothalamic NO pathway as opposed to HD apelin, we investigated the effect of HD apelin in eNOS KO mice or L-NMMA i.c.v. treated normal NC mice. In fed eNOS KO mice, i.c.v. HD apelin increased peripheral glycemia (Fig. 9G) without modification of plasma insulin (15.7 ± 4.0 vs. $22.9 \pm 6.0\,\mu$U/mL at t30; 9.8 ± 1.7 vs. $14.3 \pm 4.2\,\mu$U/mL at t15; 7.6 ± 1.4 vs. $11.7 \pm 4.3\,\mu$U/mL at t120; control vs HD apelin; $n = 12$ vs. $n = 6$, respectively). Glucose and insulin tolerance were not modified by acute i.c.v. HD apelin in eNOS KO mice and NO release in fed conditions was unchanged (data not shown). This suggests first that the hyperglycemic effects are NO-independent, and second, that in the fed state basal hypothalamic NO is sufficient to counteract the hyperglycemic effects of HD apelin in normal mice. Importantly, and in agreement with measurements made in the eNOS KO mice, HD apelin moderately increased peripheral glycemia in L-NMMA i.c.v. treated fed mice (Fig. 9H) without modification of plasma insulin (10.2 ± 2.3 vs. $5.1 \pm 0.7\,\mu$U/mL at t30; 8.3 ± 1.4 vs. $8.3 \pm 1.5\,\mu$U/mL at t15; 5.7 ± 1.0 vs. $9.3 \pm 1.6\,\mu$U/mL at t120; control vs HD apelin; $n = 5$ vs. $n = 11$, respectively), corroborating the existence of a second, distinct NO-independent pathway mediating the HD apelin effects. All other parameters (glucose/Insulin tolerance, NO release in fed conditions) were not modified by acute i.c.v. HD apelin (data not shown).

Effect of i.c.v. chronic HD apelin injection on peripheral glucose metabolism in physiological conditions

Marked elevations in the circulating concentrations of insulin and leptin are considered hallmarks of the obese and diabetic condition. Diet-induced obese mice exhibit a parallel and marked increase in plasma apelin and obese/diabetic state was associated with a chronic administration of apelin (Fig. 4). In order to assess the potential effects of a continuous priming of apelin in the brain, we assessed the effect of a 2-week continuous i.c.v. HD apelin perfusion on glucose homeostasis parameters. Body weight (26.0 ± 0.4 vs. 26.4 ± 0.3 g at week 1; 26.5 ± 0.4 vs. 26.4 ± 0.4 g at week 2, control vs chronic HD apelin; $n = 6$ vs. $n = 7$, respectively) and food intake (13.9 ± 0.4 vs. 14.2 ± 0.2 kcal/day/mouse at week 1; 15.7 ± 0.3 vs. 16.1 ± 0.6 kcal/day/mouse at week 2, control vs chronic HD apelin; $n = 6$ vs. $n = 7$, respectively) did not vary in chronic HD apelin-treated mice. In fasted state, glycemia and insulinemia significantly increased at week 2 of chronic HD apelin treatment (Figs. 10A and 10B). Fed glycemia and insulinemia did not change during the 2-weeks of experiment (Figs. 10C and 10D), corroborating the acute effect previously observed on fed state. Mice treated with HD apelin showed a significant decrease in insulin tolerance compared to control mice (Fig, 10F), reinforcing the negative impact of HD apelin in the brain.

Discussion

The brain, and more precisely the hypothalamus, is perhaps the primary orchestrator of whole body fuel sensing (26). We demonstrate here for the first time that hypothalamic apelin controls glucose homeostasis in physiological and physiopathological states. The beneficial effects of LD apelin in the hypothalamus are NO dependent, as opposed to HD apelin. In fact, our results exhibit a dose-dependent divergence in net metabolic consequence. Thus, our data suggest elevated hypothalamic apelin as a potential mediator of the diabetic state (Fig. 11).

One of the major peripheral effectors of apelin function is eNOS. The apelin/eNOS axis is represented in numerous physiological processes including vascular functions (45, 50) and peripheral glucose utilization (12), and not surprising perturbation of the axis is associated with both hypertension and diabetes, respectively. Using pharmacological and transgenic approaches, we demonstrate that NO is implicated in hypothalamic LD apelin-driven signaling effects. The observed NO release measurements (nanomolar concentrations) lie within the physiological range and are consistent with previously published functions of NO (29). Consistent with the observed effects, both constitutively expressed forms of NOS (nNOS and eNOS) are found in the hypothalamus. Also, both forms have previously been shown to be capable of modulating the central tone of glucose homeostasis (6, 16). Here, we demonstrate that beneficial effect of i.c.v. LD apelin implies an increase phosphorylation of eNOS only in fed conditions. Moreover, our finding that eNOS KO mice do not respond to i.c.v. LD apelin supports a dominant role for the eNOS isoform in the apelin-driven effects. We cannot rule out the fact that one characteristic of eNOS KO mice is to present a clear insulin-resistant state and the absence of i.c.v. LD apelin effect could be related to peripheral disturbance. Conversely to this hypothesis, eNOS KO mice are still able to response to i.c.v. SNAP by an increase in insulinemia as previously observed in a rat model in which hypothalamus is stimulated by intracarotid NO donor (27). In spite of a lack of clear amelioration of glucose tolerance, eNOS KO mice present a more rapid return to normal glycemia (from t60 to t120, Fig. 9A). All these data suggest that the brain of eNOS KO mice can response to NO donor with peripheral physiological changes. We can speculate that these modifications can be amplifying in response to higher (supraphysiological) doses of i.c.v. NO donor.

Interestingly, when challenged with HD central apelin, both eNOS KO and L-NMMA treated mice present an increase in glycemia in the fed state. These findings suggest that a basal tone of NO in the hypothalamus is crucial for the maintenance of a physiological glycemia, and NO from endothelial origin is implicated in the hypoglycemic effect of apelin. This hypothesis is supported by the work of Shankar *et al*. (36) demonstrating that i.c.v. L-NMMA injection in the rat increases insulin resistance. Finally, *ex vivo* hypothalami

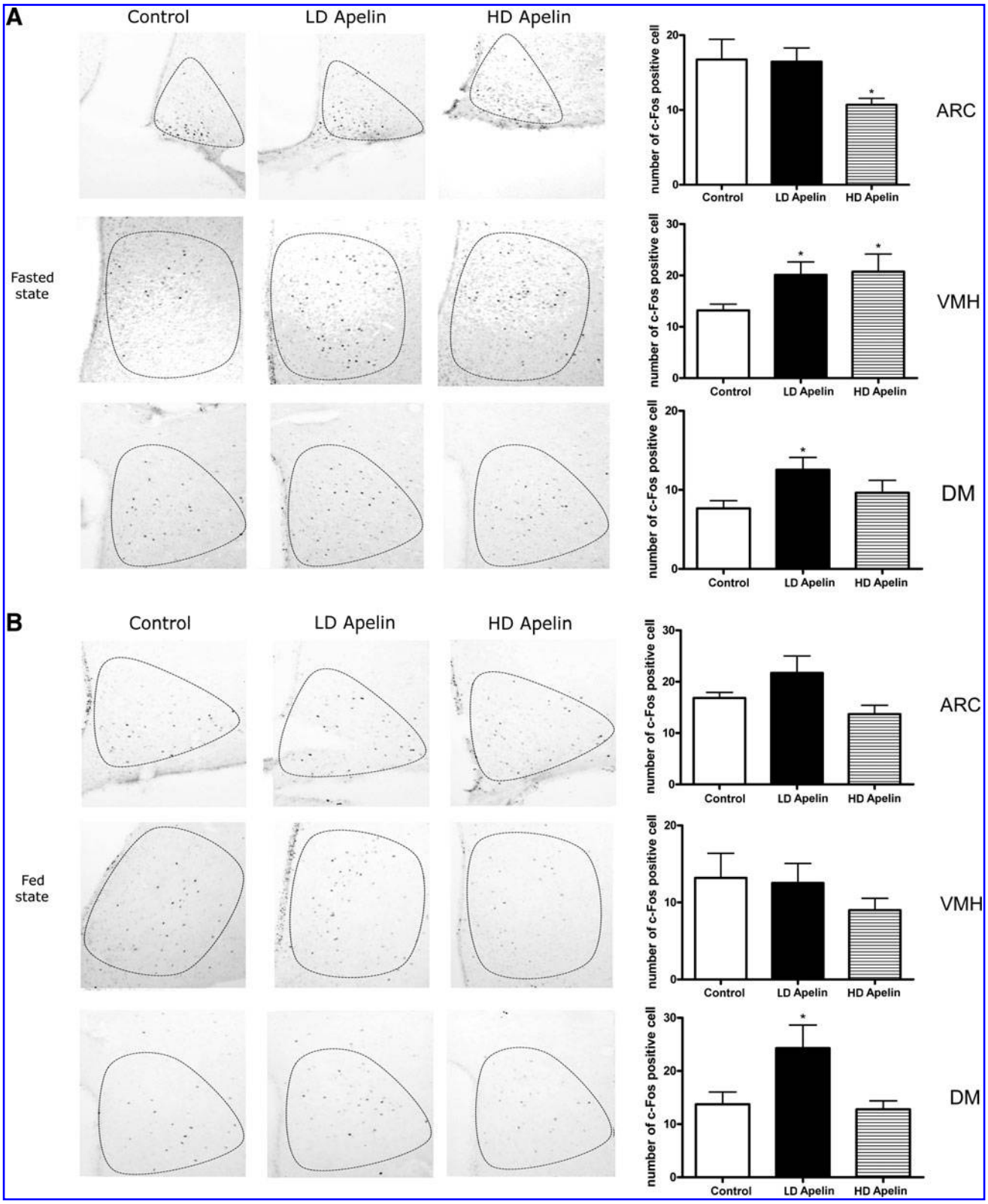

FIG. 7. Differential c-Fos activation by i.c.v. LD or HD apelin in the hypothalamus. (A) Representative staining of c-Fos-expressing cells in the ARC, VMH, and DM nuclei after i.c.v. injection of LD apelin ($n=4$), HD apelin ($n=4$), or aCSF ($n=4$) in fasted NC WT mice. Means ± SEM are represented in a graph; *$p<0.05$ versus aCSF. **(B)** Representative staining of c-Fos-expressing cells in the ARC, VMH, and DM nuclei after i.c.v. injection of LD apelin ($n=4$), HD apelin ($n=4$), or aCSF ($n=4$) in fed NC WT mice; *$p<0.05$ versus aCSF. Results are the mean ± SEM.

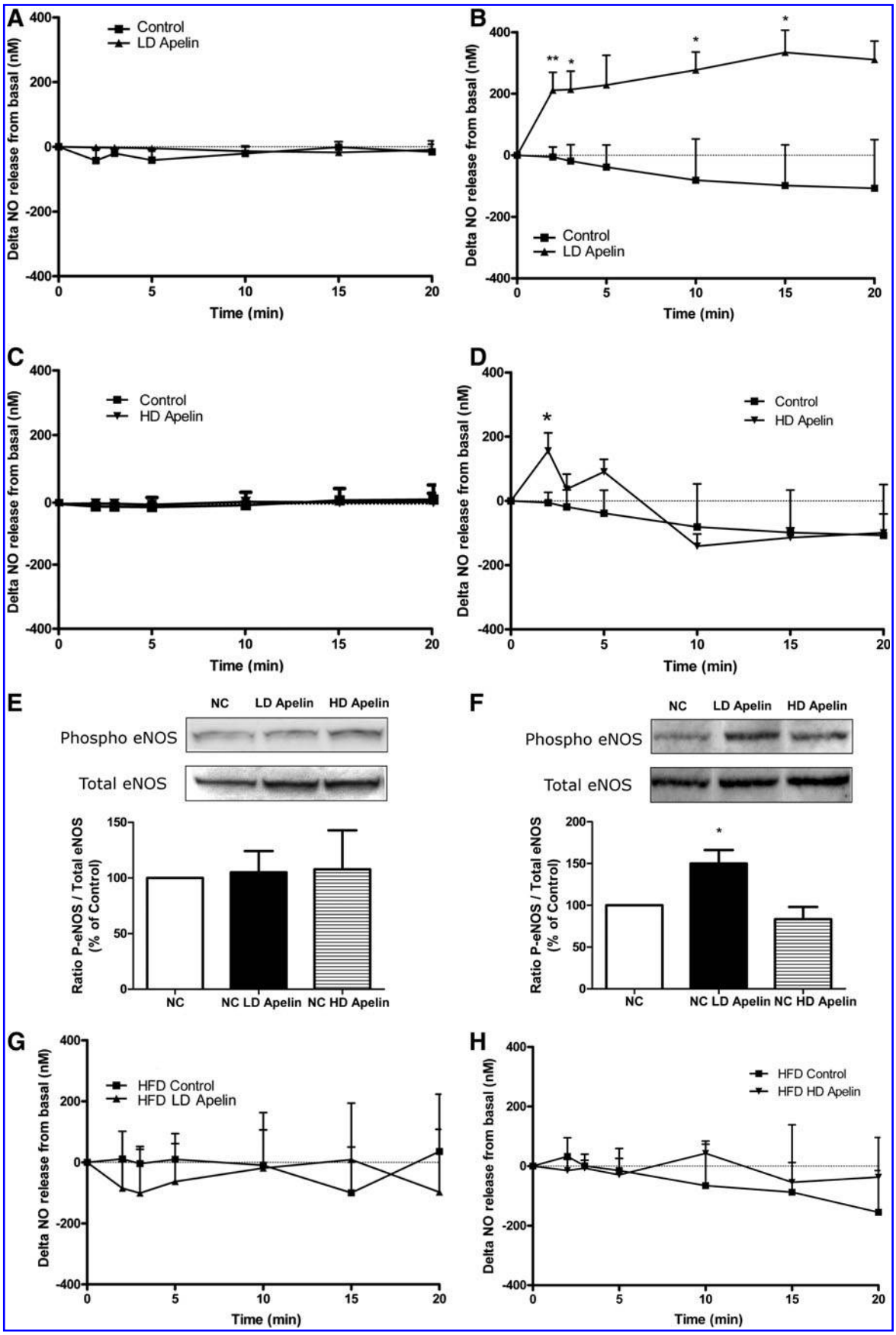
A
Control
LD Apelin
Delta NO release from basal (nM)
Time (min)
B
Control
LD Apelin
Delta NO release from basal (nM)
Time (min)
C
Control
HD Apelin
Delta NO release from basal (nM)
Time (min)
D
Control
HD Apelin
Delta NO release from basal (nM)
Time (min)
E
NC
LD Apelin
HD Apelin
Phospho eNOS
Total eNOS
Ratio P-eNOS / Total eNOS (% of Control)
NC
NC LD Apelin
NC HD Apelin
F
NC
LD Apelin
HD Apelin
Phospho eNOS
Total eNOS
Ratio P-eNOS / Total eNOS (% of Control)
NC
NC LD Apelin
NC HD Apelin
G
HFD Control
HFD LD Apelin
Delta NO release from basal (nM)
Time (min)
H
HFD Control
HFD HD Apelin
Delta NO release from basal (nM)
Time (min)

treated with HD apelin did not exhibit increased NO release throughout the 20 minutes of exposure, suggesting that HD apelin activates inhibitory signals for NO. In contrast to LD apelin, we hypothesize that HD apelin may decrease NO release in hypothalamic explants, as observed with leptin on pituitary cells (25). This hypothesis supposes that high levels of hypothalamic apelin are able to stimulate inhibitory factors of NOS activity such as beta-endorphin (15) or of eNOS cofactors such as reactive oxygen species (20). In support of such a mechanism, we have observed that HD apelin stimulates hydrogen peroxide release from *ex vivo* hypothalamus (data not shown). The fact that HD apelin did not increase the phosphorylation of eNOS in fed conditions as opposed to LD apelin, further reinforce this hypothesis. An equally plausible hypothesis would be that the APJ receptor-induced signaling cascade exhibits desensitization in response to HD apelin. Indeed, i.c.v. apelin has been shown to induce a downregulation of the receptor itself in the hypothalamus of HFD mice (8).

We hypothesized that elevated levels of central apelin might impair glucose homeostasis since obese/diabetic mice, which are sensitive to peripheral apelin (12), present increased plasma apelin levels. Both the finding of abolished circadian apelin regulation in HFD-treated mice (Fig. 4) and that of chronic apelin triggering insulin intolerance (Fig. 9) are consistent with this hypothesis. Interestingly, the finding that HD central apelin increases blood glucose during fasting (Fig. 5) suggests a link between central apelin and the control of hepatic glucose production. Although hepatic glucose production was not significantly modified during the clamp, a link between central apelin and liver could be suggested since HD apelin increases blood glucose during fasting. Numerous studies have implicated the autonomous nervous system in the central control of liver glucose metabolism. Indeed, hepatic denervation (48) and electrical stimulation (38) modify glycogen liver content. Also, the stimulation of the VMH produces hyperglycemia by increasing glycogenolysis and gluconeogenesis (9) which are mediated by sympathetic efferents. Importantly, the previously described kinetics of sympathetic gluco-regulation (glycogenolysis within minutes; gluconeogenesis within hours) (39–41) clearly fits with our observation of two waves of increased glucose release after HD apelin. While these hepatic gluco-regulatory effects and the c-Fos staining profiles (Fig. 7) clearly highlight an activity of apelin at the VMH, the concurrent capacity of apelin to initiate insulin release suggests the additional involvement of parasympathetic regulation and thus of additional hypothalamic nuclei (the lateral hypothalamus and periventricular hypothalamic nucleus). Such a concept could explain the dose dependency of apelin action and places the apelin/APJ axis as a novel central regulator of glucose homeostasis. In accordance with this hypothesis, we found that i.c.v. apelin differentially affects glucose metabolism. LD apelin improve fed glycemia and glucose tolerance. In fasted state, LD apelin did not changes glycemia, while supraphysiological insulin stimulation increased insulin tolerance. To verify this hypothesis, we performed euglycemic-hyperinsulinemic clamp studies and did not find any modification of glucose turnover. Therefore, this suggests that in the fasted state, the brain cannot adequately respond to LD apelin as opposed to a hyperglycemic state. Interestingly, HD apelin markedly increased plasma insulin secretion during fasted state and oral glucose load. This last observation suggests that HD apelin promotes a moderate insulin resistance state. Nonetheless, we did not find any changes of insulin tolerance upon ITT, however, we may not rule out that the supraphysiological dose of insulin used exceeds the physiological impact of i.c.v. HD apelin, thereby jeopardizing the real assessment of insulin sensitivity. Therefore, we decided to investigate insulin sensitivity by using the gold standard method, namely the euglycemic-hyperinsulinemic clamp studies. Importantly, by using this method, we found that HD apelin administration promotes whole body insulin resistance.

Although i.c.v. apelin controls peripheral glucose homeostasis, chronic i.c.v. perfusion of apelin does not modify cumulative food intake in our experiment. This result is in accordance with Taheri *et al*. (44) which demonstrates similar effect in rats. At the opposite, numerous studies implicate central apelin as a positive (47) or negative regulator (43) of food intake. Such discrepancies could be explain by injection process (acute vs. chronic), the dose injected in lateral ventricle (low vs. high) and by the nutritional state (fast vs. fed) (44). In our study, we demonstrate that LD apelin targets hypothalamic NO in fed conditions. One of the mechanisms could be explained by the fact that the hypothalamus needs an impregnation of peripheral factors (including glucose and/or insulin) to adequately respond to brain apelin via NO. In accordance with this hypothesis, Becskei *et al*. (2) demonstrate a differential expression of c-Fos expression in the arcuate nucleus of fasted, chow-refed or *ad libidum* fed mice associated to variations of plasma hormones concentrations (insulin, leptin, ghrelin). In this study, the authors also demonstrate that supplementation of food with macronutrients (protein, fat, or carbohydrates) may modify c-Fos expression in refeeding mice, suggesting that the arcuate nucleus represents an important site in the short-term control of energy intake. However, the feeding-related factors implicated in the genesis of the transition from fasted to fed state in the hypothalamus,

FIG. 8. i.c.v. LD apelin targets eNOS in the hypothalamus. (A) *Ex vivo* hypothalamic NO release measured by real-time amperometric detection in fasted NC WT mice after injection of LD apelin ($n=5$) or aCSF ($n=6$). **(B)** *Ex vivo* hypothalamic NO release measured by real-time amperometric detection in fed NC WT mice after injection of LD apelin ($n=5$) or aCSF ($n=6$); $^{*}p<0.05$, $^{**}p<0.01$. **(C)** *Ex vivo* hypothalamic NO release measured by real-time amperometric detection in fasted NC WT mice after injection of HD apelin ($n=4$) or aCSF ($n=5$). **(D)** *Ex vivo* hypothalamic NO release measured by real-time amperometric detection in fed NC WT mice after injection of HD apelin ($n=6$) or aCSF ($n=6$); $^{*}p<0.05$. **(E)** Representative blots and quantification of eNOS expression (phosphorylated and total forms) in *ex vivo* hypothalamus of fasted NC mice incubated with saline, LD apelin, or HD apelin ($n=4$). **(F)** Representative blots and quantification of eNOS expression (phosphorylated and total forms) in *ex vivo* hypothalamus of fed NC mice incubated with saline, LD apelin, or HD apelin ($n=4$); $^{*}p<0.05$. **(G)** *Ex vivo* hypothalamic NO release measured by real-time amperometric detection in fed HFD WT mice after injection of LD apelin ($n=5$) or aCSF ($n=6$). **(H)** *Ex vivo* hypothalamic NO release measured by real-time amperometric detection in fed HFD WT mice after injection of HD apelin ($n=5$) or aCSF ($n=6$). Results are the mean ± SEM.

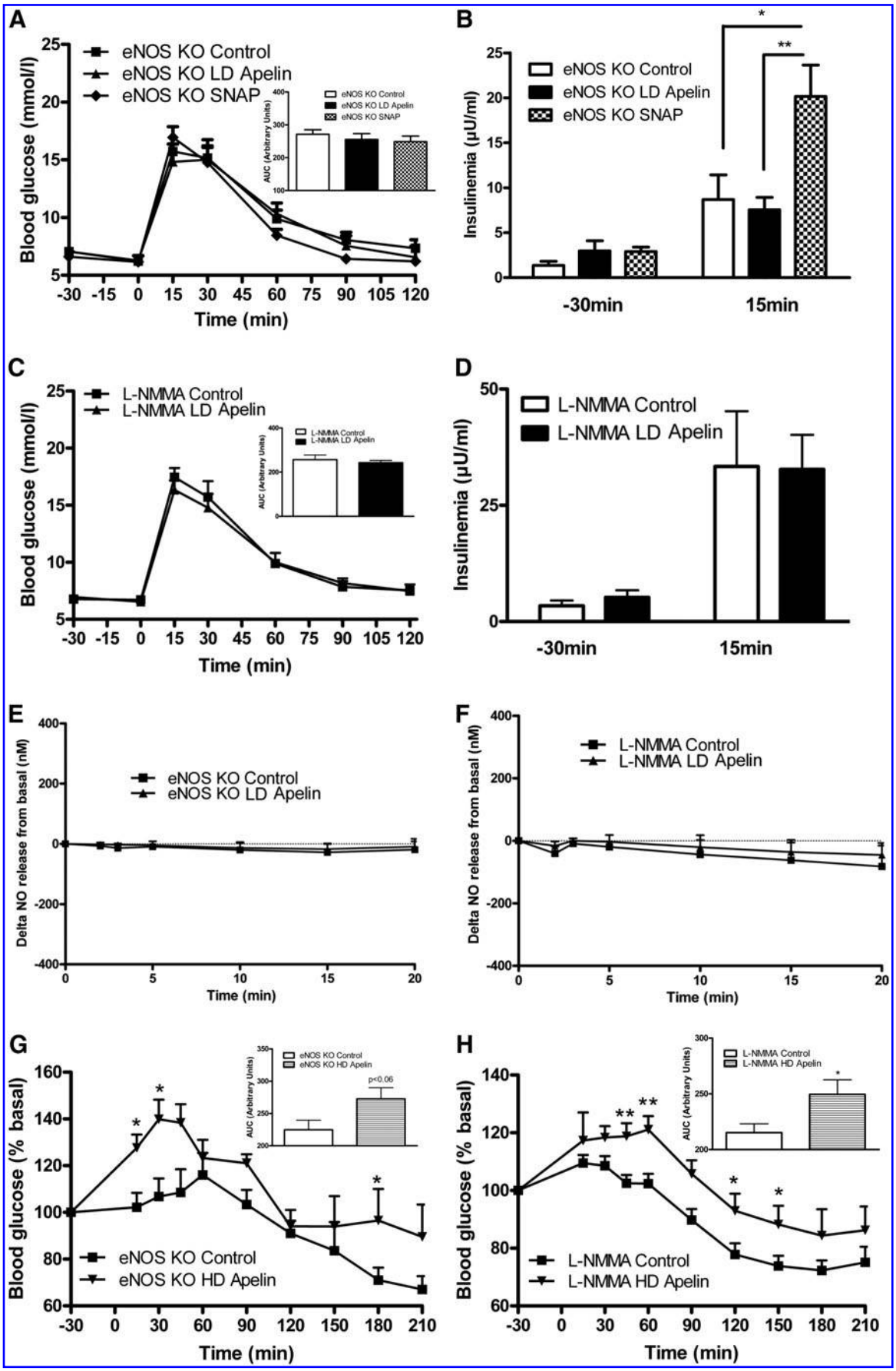
A
eNOS KO Control
eNOS KO LD Apelin
eNOS KO SNAP
Blood glucose (mmol/l)
Time (min)
AUC (Arbitrary Units)
B
Insulinemia (µU/ml)
-30min
15min
C
L-NMMA Control
L-NMMA LD Apelin
D
E
Delta NO release from basal (nM)
F
G
eNOS KO HD Apelin
p<0.06
Blood glucose (% basal)
H
L-NMMA HD Apelin

and thus contributing to the brain apelin/NO effect during fed state, remain to be defined. Thus, we can speculate that the capacity of hypothalamic nuclei to respond to apelin varied in function of numerous parameters, including the nutritional state as suggested by our c-Fos study in the hypothalamus and by plasma apelin variations observed during the day. Such variations of hypothalamic c-Fos expression during the nutritional state and/or apelin levels may have consequence on autonomous nervous system activity which could explain peripheral variations observed on glycemia and insulin release. Thus, we can speculate that such a modification of hypothalamus activity in our model may have consequences on glucose homeostasis, and identification of apelinergic neurons and efferent nervous signals implicated in this control need to be further explored.

This study shows for the first time that centrally injection of apelin modulates glucose homeostasis. The downstream effects are pleiotropic, dose-dependent, and involve several distinct hypothalamic nuclei that link hepatic glucose production, insulin release, and centers mediating autonomic control. Finally, results including generation of a central apelin-resistant state *in vivo* reveal apelin/APJ as a novel mechanistic candidate for the transition from normal to diabetic states. In fact, potential therapeutic strategies based on apelin/APJ system have to preferentially target peripheral apelin effects since they are conserved in HFD mice model (12). Evaluation of the quantity of iv apelin able to reach the brain while retaining beneficial peripheral effect on glycemia will be a major issue for the future clinical relevance of apelin.

Materials and Methods

Mice

Animals were handled in accordance with the principles and guidelines established by the National Institute of Medical Research (INSERM) and by the local ethical committee of the IFR-BMT. C57Bl6/J mice and mice deficient in endothelial NO synthase (eNOS -/-) on a C57Bl6/J background were obtained from Charles River Laboratory (l'Arbresle, France). Mice were housed conventionally in a constant temperature (20°–22°C) and humidity (50%–60%) animal room and with a 12/12h light/dark cycle (lights off at 7:00 AM) and free access to food and water through the 24 h period. All injections and experiments were performed in 13–15-week-old males. A group of male mice was subjected to high fat diet (HFD) containing 20% protein, 35% carbohydrate, and 45% fat (SAFE, Augy, France). HFD-fed mice were followed at regular intervals with measure of weight and blood parameters (glucose, insulin) until they were obese and insulin resistant corresponding to 3 months of HFD. Experiments were performed on 6 h-fasted or fed mice. During the time of experiment (3 hours), mice fed overnight were placed in a new clean cage without food.

Surgical procedures

For *in vivo* acute and chronic perfusions, an indwelling i.c.v. catheter (Alzet Brain Perfusion Kit 3, 1-3 mm, Charles River, 0.1 mm lateral, 0.22 mm anteroposterior from the bregma and 1.5 mm deep) was implanted in anesthetized mice with isoflurane (Abbott, Ringis, France). For chronic perfusions, the i.c.v. catheter was connected to an osmotic mini-pomp (Model 2004, Alzet; Cupertino, CA), as previously described (21).

Acute injections

Apelin. Bolus injection of 2 μl of [Pyr]apelin-13 (concentration from 10 p*M* to 50 n*M* corresponding to 20.10^{-3} fmol to 50 fmol, Bachem, UK), the most active apelin isoform (12), was injected directly to the i.c.v. catheter completed to 2 μl of artificial cerebrospinal fluid (aCSF) for treated mice, or 4 μl of aCSF for control mice. Blood glycemia was measured every 30 min from −30 to 210 min (time 0 corresponding to i.c.v. apelin injection). To limit stress due to accumulation of tail blood samples, insulinemia was measured at different time intervals from −30 to 120 min in another set of mice.

NOS inhibitor. Similar experiments were performed with a NOS inhibitor, *N*G-monomethyl-L-arginine (L-NMMA, Sigma), who was dissolved extemporaneously in aCSF, and then infused at a concentration of 100 μM (2 μl). The L-NMMA infusion was started 30 min before the start of the apelin injection.

Chronic perfusion of apelin

Using an osmotic mini-pump system connected to the lateral ventricle, we measured glucose homeostasis parameters, as previously described in detail (21). Briefly, the osmotic mini-pump delivers either aCSF or apelin-13 (high-dose, HD; 2 μl of 20 n*M*) over 2 weeks, at a rate of 0.25 μl/h. Fasted/fed glycemia and insulinemia, body weight, and food intake were evaluated every week. In a different set of mice, ITT were performed during the treatment.

FIG. 9. Genetic deletion of eNOS or pharmacological blockade of NOS affects i.c.v. LD apelin but not HD apelin effect on glucose homeostasis. (A) OGTT in 6-hour-fasted NC eNOS KO mice i.c.v. injected with LD apelin ($n=7$), the NO donor SNAP ($n=9$), or aCSF ($n=6$). The *adjacent bar graph* represents the average AUC. **(B)** OGTT-associated insulinemia in 6-hour-fasted NC eNOS KO mice i.c.v. injected with LD apelin (*black*, $n=7$), SNAP (*hatched*, $n=9$), or aCSF (*white*, $n=6$); $^*p<0.05$ eNOS KO SNAP vs. eNOS KO Control and $^{**}p<0.01$, eNOS KO SNAP vs. eNOS KO LD apelin following one-way ANOVA analysis, followed by Bonferoni's *post-hoc* test. **(C)** OGTT in 6-hour-fasted NC WT mice treated with L-NMMA and i.c.v. injected with LD apelin ($n=7$) or aCSF ($n=7$). The *adjacent bar graph* represents the average AUC. **(D)** OGTT-associated insulinemia in 6-hour-fasted NC WT mice treated with L-NMMA and i.c.v. injected with LD apelin (*black*, $n=7$) or aCSF (*white*, $n=7$). **(E)** *Ex vivo* hypothalamic NO release measured by real-time amperometric detection in fed NC eNOS KO mice after injection of LD apelin ($n=6$) or aCSF ($n=5$). **(F)** *Ex vivo* hypothalamic NO release measured by real-time amperometric detection in fed NC WT mice treated with L-NMMA after injection of LD apelin ($n=5$) or aCSF ($n=5$). **(G)** Effect of acute i.c.v. injection of HD apelin ($n=6$) on blood glucose in fed NC eNOS KO mice compared to aCSF injected fed NC eNOS KO mice ($n=11$). The *adjacent bar graph* represents the average AUC; $^*p<0.05$. **(H)** Effect of acute i.c.v. injection of HD apelin ($n=11$) on blood glucose in fed NC WT mice treated with L-NMMA compared to aCSF injected fed NC WT mice treated with L-NMMA ($n=18$). The *adjacent bar graph* represents the average AUC; $^*p<0.05$, $^{**}p<0.01$. Results are the mean ± SEM.

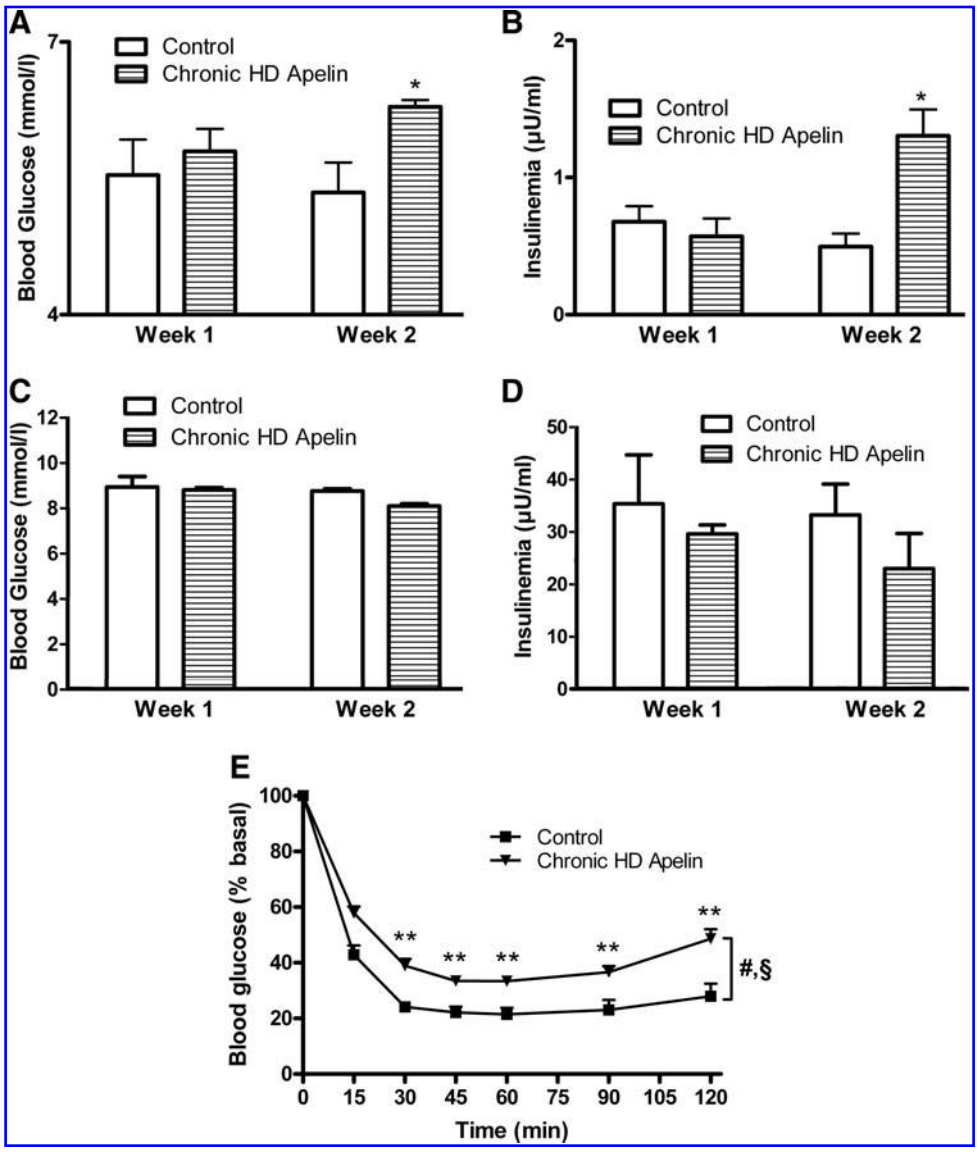

FIG. 10. Chronic i.c.v. HD apelin perfusion alters glucose metabolism in NC mice. (A) 2 weeks time-course blood glucose in fasted NC WT mice with chronic i.c.v. perfusion of HD apelin (*hatched*, $n=7$) or aCSF (*white*, $n=6$); $^{*}p<0.05$. **(B)** 2 weeks time-course insulinemia evolution in fasted NC WT mice with chronic i.c.v. infusion of HD apelin (*hatched*, $n=7$) or aCSF (*white*, $n=6$); $^{*}p<0.05$. **(C)** 2 weeks time-course blood glucose in fed NC WT mice with chronic i.c.v. perfusion of HD apelin (*hatched*, $n=7$) or aCSF (*white*, $n=6$). **(D)** 2 weeks time-course insulinemia evolution in fed NC WT mice with chronic i.c.v. infusion of HD apelin (*hatched*, $n=7$) or aCSF (*white*, $n=6$). **(E)** ITT in 6-hour-fasted NC WT mice with chronic i.c.v. infusion of HD apelin ($n=6$) or aCSF ($n=6$); $^{*}p<0.05$, $^{**}p<0.01$. Two-way ANOVA followed by *t*-test *post hoc* reveals time ($^{\#}p<0.001$) and treatment ($^{\S}p<0.001$) effects. Results are the mean ± SEM.

Real-time amperometric NO measurements

Mice were decapitated without anesthesia after 6 hours of fasting or fed conditions. After dissection, hypothalamus fragment was washed in Krebs-Ringer bicarbonate/glucose buffer (pH 7.4) in an atmosphere of 95% O_2–5% CO_2 and then immersed in Eppendorf tubes containing 400 μl of the same medium. Each tube contained one hypothalamus. After a 10 min recovery period, the spontaneous NO release was measured at 35°C for 20 min by using a NO-specific amperometric probe (ISO-NOPF, 100 μm diameter, 5 mm length, World Precision Instruments, Aston Stevenage, UK) implanted directly in the hypothalamus (13, 16). Apelin-13 or saline was injected directly in the survival medium (final concentrations: 10 p*M* or 20 n*M*). Calibration of the electrochemical sensor was performed by the use of different concentrations of a nitrosothiol donor S-nitroso-*N*-acetyl-D,L-penicillamine (SNAP, Sigma), as previously described in details (16, 24). The concentration of NO gas in solution was measured in real-time with data acquisition (Apollo1000, World Precision Instruments, Aston Stevenage, UK) at a sampling rate of 10 values/sec. The computer-interfaced DataTrax2 software (World Precision Instruments, Aston Stevenage, UK) performed data acquisition. Data are expressed as delta variation of NO release from basal.

Oral glucose tolerance test

6 hour-fasted mice were injected with i.c.v. apelin-13 or aCSF 120 min before oral glucose (3 g/kg) loading. Blood was collected from the tail vein at −30, 0, 15, 30, 45, 60, 90, and 120 min later for determination of glucose levels. Blood was also collected 30 min before and after 15 min glucose loading for determination of plasma insulin concentration, as previously described (21–23). In another set of mice, pharmacological blockade of NOS was induced by i.c.v. L-NMMA injection 150 min before apelin treatment, and consequences on glycemia and insulinemia were measured. In a similar way, experiments were performed in the presence of the NO donor SNAP (S-nitroso-*N*-acetyl-D,L-penicillamine, Sigma) that was dissolved extemporaneously in aCSF, and then infused at a dose of 22.7 nmol in 2 μl completed to 2 μl of aCSF in

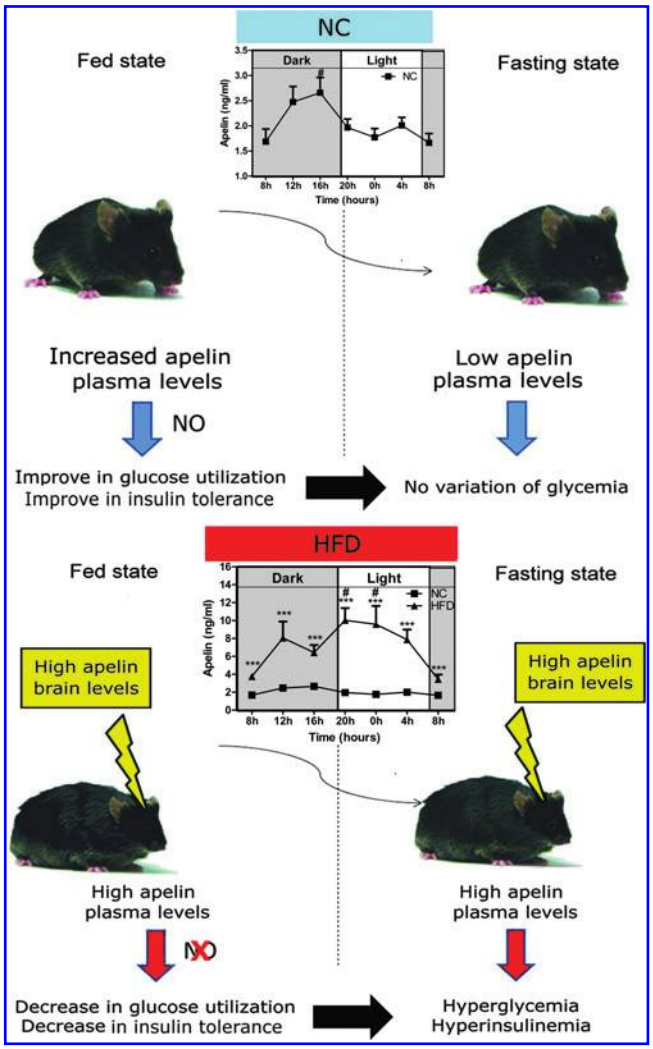

FIG. 11. Apelin mediates the transition from normal to the diabetic state. In the physiological fed state, the increase in plasma apelin levels exerts beneficial effects on peripheral glycemia. In the physiopathological state, the high plasma apelin levels may exert deleterious effects in the brain, resulting in hyperglycemia and hyperinsulinemia in fasted conditions, suggesting a novel role of apelin mediating the transition from normal to the diabetic state.

eNOS KO mice. At this dose, i.c.v. SNAP did not modify peripheral plasma concentrations of hormones including angiotensin II and vasopressin (34). SNAP infusion was started 120 min before oral glucose (3 g/kg) loading.

ITT

6 hour-fasted mice were injected with i.c.v. apelin-13 or aCSF 120 min before intraperitoneal insulin injection (1 mU/g), as previously described (46). Blood was collected from the tail vein at −30, 0, 15, 30, 45, 60, 90, and 120 min later for determination of glucose levels.

Euglycemic hyperinsulinemic clamp

A femoral iv catheter was implanted 7 days before clamp studies. Hepatic glucose production (HGP) and whole body glucose turnover (TO) were evaluated by the hyperinsulinemic-euglycemic clamp technique, conducted at a 6-h fast with a continuous infusion of 2.5 mU/kg^{-1}/min^{-1} human insulin (Actrapid) coupled with [3-^{3}H]glucose (0.33 μCi, PerkinElmer, Boston, MA). 6 hour-fasted mice were injected with i.c.v. apelin-13 or aCSF before starting the clamp, as previously described (23). Tail blood glycemia was obtained at time 0 and every 10 min thereafter to adjust a variable 20% glucose infusion rate (GIR) to maintain euglycemia (5–6 m*M*). When steady-state was obtained (±90 min), blood samples (5 μl) were collected every 10 min for 1 h for estimation of plasma glucose specific activity. At steady state, the rate of glucose appearance (Ra) measured as = [3-^{3}H]GIR/glucose specific activity equals the rate of peripheral glucose disposal (Rd) or TO. In insulin-stimulated conditions (2.5mU/kg^{-1}/min^{-1}), HGP was obtained by subtracting the GIR (mg/kg^{-1}/min^{-1}) to the Rd previously calculated: HGP (Ra) = Rd - GIR. The whole-body glycolytic flux was calculated from the [^{3}H]$_2$O accumulated in the plasma during the last hour of the infusions. The whole-body glycogen synthesis (Gln Synth) rate was calculated by subtracting the glycolytic flux (glycolysis, glycol) from the glucose turnover rate. For each mouse, the mean values have been calculated and then averaged with values from mice from the same group.

Insulin assays

Serum insulin was measured using an ultra-sensitive mouse insulin ELISA (Mercodia, Uppsala, Sweden).

Variations of plasma apelin levels

Plasma apelin levels for NC and HFD mice were measured every 4 hours with a commercially available enzyme-linked immunoassay (ELISA) kit (Phoenix Pharmaceuticals, Burlingame, CA). The sensitivity of the assay was 0.2 ng/ml and the intra-assay error was below 5%. The ELISA had 100% cross-reactivity with human apelin-12, apelin-13, and apelin-36.

Quantification of c-Fos expression in the hypothalamus

A bolus injection of 2 μl of Apelin-13 was performed as described above. Mice were anesthetized 2 h after the injection, perfused with 4% picric acid buffer and 4% formaldehyde. The brain was removed from the skull, postfixed with the formaldehyde buffer, cryoprotected one night in 20% sucrose, sectioned, and stained for immunohistochemistry, as previously described in detail (22).

Western blot analysis

Mice were decapitated without anesthesia after 6 hours of fasting or in fed conditions. After dissection, the hypothalamus fragment was washed in Krebs-Ringer bicarbonate/glucose buffer (pH 7.4) in an atmosphere containing 95% O_2–5% CO_2 and then immersed in tubes containing 400 μl of the same medium. Each tube contained one hypothalamus. Apelin-13 or saline was injected directly in the survival medium (final concentrations: 10 p*M* or 20 n*M*). After 3 min of incubation, each hypothalamus was frozen at –80°C in liquid nitrogen and homogenized in lysis buffer. Then, blots were performed as previously described (6). Briefly, the membranes were blocked for 90 min at room temperature with 5% dried milk and incubated overnight at 4°C with a primary

polyclonal antibody against total eNOS (dilution 1/1,000; Santa Cruz Biotechnology, Santa Cruz, CA) or the phosphorylated active form (Ser1177) of eNOS (dilution 1/1,000; Cell Signaling Technology, Ozyme, St. Quentin Yvelines, France). After three washes, membranes were incubated with horseradish peroxidase-conjugated anti-rabbit IgG antibody (dilution 1/10,000; Amersham Biosciences Europe, Orsay, France) for 2 hours. Immunoreactivity was detected using an enhanced chemiluminescence detection kit (ECL system; Amersham Biosciences Europe) and exposure to X-ray film (Amersham Hyperfilm ECL, GE Health Care Bio-Sciences Corp, Piscataway, NJ). Bands were quantified using Image Quant system (GE Health Care Bio-Sciences Corp). Data are expressed as percentage of variations of ratio phosphorylated protein/total protein compared to control.

Statistical analysis

Results are presented as mean ± SEM. The statistical significance of differences was analyzed by student *t*-test, by two-way ANOVA followed by a *post hoc t*-test, or one-way followed by *post-hoc* Bonferroni's or Dunnett's multiple comparison test, when appropriate. Statistical analyses were assessed by using GraphPad Prism version 5.00 for windows (GraphPad Software, San Diego, CA). Results were considered statistically significant when $p < 0.05$.

Acknowledgments

PDC is research associate from the FRS-FNRS (Fonds de la Recherche Scientifique) Belgium. This work was supported by the "Société Française de Nutrition" (SFN). We thank Pr Jean-François Arnal for eNOS KO mice generous gift, Amandine Everard from UCL and the "Plateforme Genotoul Anexplo" from Toulouse for excellent technical assistance. We thank Nadia De Mota for technical advice.

Author Disclosure Statement

No competing financial interests exist.

References

1. Ahima RS and Osei SY. Adipokines in obesity. *Front Horm Res* 36: 182–197, 2008.
2. Becskei C, Lutz TA, and Riediger T. Diet-derived nutrients mediate the inhibition of hypothalamic NPY neurons in the arcuate nucleus of mice during refeeding. *Am J Physiol Regul Integr Comp Physiol* 297: R100–110, 2009.
3. Boucher J, Masri B, Daviaud D, Gesta S, Guigne C, Mazzucotelli A, Castan-Laurell I, Tack I, Knibiehler B, Carpene C, Audigier Y, Saulnier-Blache JS, and Valet P. Apelin, a newly identified adipokine up-regulated by insulin and obesity. *Endocrinology* 146: 1764–1771, 2005.
4. Burcelin R, Cani PD, and Knauf C. Glucagon-like peptide-1 and energy homeostasis. *J Nutr* 137: 2534S–2538S, 2007.
5. Cabou C, Campistron G, Marsollier N, Leloup C, Cruciani-Guglielmacci C, Penicaud L, Drucker DJ, Magnan C, and Burcelin R. Brain glucagon-like peptide-1 regulates arterial blood flow, heart rate, and insulin sensitivity. *Diabetes* 57: 2577–2587, 2008.
6. Cabou C, Cani PD, Campistron G, Knauf C, Mathieu C, Sartori C, Amar J, Scherrer U, and Burcelin R. Central insulin regulates heart rate and arterial blood flow: An endothelial nitric oxide synthase-dependent mechanism altered during diabetes. *Diabetes* 56: 2872–2877, 2007.
7. Carpene C, Dray C, Attane C, Valet P, Portillo MP, Churruca I, Milagro FI, and Castan-Laurell I. Expanding role for the apelin/APJ system in physiopathology. *J Physiol Biochem* 63: 359–373, 2007.
8. Clarke KJ, Whitaker KW, and Reyes TM. Diminished metabolic responses to centrally-administered apelin-13 in diet-induced obese rats fed a high-fat diet. *J Neuroendocrinol* 21: 83–89, 2009.
9. Corssmit EP, Romijn JA, and Sauerwein HP. Review article: Regulation of glucose production with special attention to nonclassical regulatory mechanisms: A review. *Metabolism* 50: 742–755, 2001.
10. De Mota N, Lenkei Z, and Llorens-Cortes C. Cloning, pharmacological characterization and brain distribution of the rat apelin receptor. *Neuroendocrinology* 72: 400–407, 2000.
11. De Mota N, Reaux-Le Goazigo A, El Messari S, Chartrel N, Roesch D, Dujardin C, Kordon C, Vaudry H, Moos F, and Llorens-Cortes C. Apelin, a potent diuretic neuropeptide counteracting vasopressin actions through inhibition of vasopressin neuron activity and vasopressin release. *Proc Natl Acad Sci USA* 101: 10464–10469, 2004.
12. Dray C, Knauf C, Daviaud D, Waget A, Boucher J, Buleon M, Cani PD, Attane C, Guigne C, Carpene C, Burcelin R, Castan-Laurell I, and Valet P. Apelin stimulates glucose utilization in normal and obese insulin-resistant mice. *Cell Metab* 8: 437–445, 2008.
13. Duparc T, Naslain D, Colom AX, Muccioli GG, Massaly N, Delzenne NM, Valet P, Cani PD, and Knauf C. Jejunum inflammation in obese and diabetic mice impairs enteric glucose detection and modifies nitric oxide release in the hypothalamus. *Antioxid Redox Signal* 14: 415–423, 2011.
14. Erdem G, Dogru T, Tasci I, Sonmez A, and Tapan S. Low plasma apelin levels in newly diagnosed type 2 diabetes mellitus. *Exp Clin Endocrinol Diabetes* 116: 289–292, 2008.
15. Faletti AG, Mastronardi CA, Lomniczi A, Seilicovich A, Gimeno M, McCann SM, and Rettori V. beta-Endorphin blocks luteinizing hormone-releasing hormone release by inhibiting the nitricoxidergic pathway controlling its release. *Proc Natl Acad Sci USA* 96: 1722–1726, 1999.
16. Fioramonti X, Marsollier N, Song Z, Fakira KA, Patel RM, Brown S, Duparc T, Pica-Mendez A, Sanders NM, Knauf C, Valet P, McCrimmon RJ, Beuve A, Magnan C, and Routh VH. Ventromedial hypothalamic nitric oxide production is necessary for hypoglycemia detection and counter-regulation. *Diabetes* 59: 519–528, 2010.
17. Frier BC, Williams DB, and Wright DC. The effects of apelin treatment on skeletal muscle mitochondrial content. *Am J Physiol Regul Integr Comp Physiol* 297: R1761–1768, 2009.
18. Heinonen MV, Purhonen AK, Miettinen P, Paakkonen M, Pirinen E, Alhava E, Akerman K, and Herzig KH. Apelin, orexin-A and leptin plasma levels in morbid obesity and effect of gastric banding. *Regul Pept* 130: 7–13, 2005.
19. Higuchi K, Masaki T, Gotoh K, Chiba S, Katsuragi I, Tanaka K, Kakuma T, and Yoshimatsu H. Apelin, an APJ receptor ligand, regulates body adiposity and favors the messenger ribonucleic acid expression of uncoupling proteins in mice. *Endocrinology* 148: 2690–2697, 2007.
20. Jaimes EA, Sweeney C, and Raij L. Effects of the reactive oxygen species hydrogen peroxide and hypochlorite on en-

dothelial nitric oxide production. *Hypertension* 38: 877–883, 2001.
21. Knauf C, Cani PD, Ait-Belgnaoui A, Benani A, Dray C, Cabou C, Colom A, Uldry M, Rastrelli S, Sabatier E, Godet N, Waget A, Penicaud L, Valet P, and Burcelin R. Brain glucagon-like peptide 1 signaling controls the onset of high-fat diet-induced insulin resistance and reduces energy expenditure. *Endocrinology* 149: 4768–4777, 2008.
22. Knauf C, Cani PD, Kim DH, Iglesias MA, Chabo C, Waget A, Colom A, Rastrelli S, Delzenne NM, Drucker DJ, Seeley RJ, and Burcelin R. Role of central nervous system glucagon-like peptide-1 receptors in enteric glucose sensing. *Diabetes* 57: 2603–2612, 2008.
23. Knauf C, Cani PD, Perrin C, Iglesias MA, Maury JF, Bernard E, Benhamed F, Gremeaux T, Drucker DJ, Kahn CR, Girard J, Tanti JF, Delzenne NM, Postic C, and Burcelin R. Brain glucagon-like peptide-1 increases insulin secretion and muscle insulin resistance to favor hepatic glycogen storage. *J Clin Invest* 115: 3554–3563, 2005.
24. Knauf C, Prevot V, Stefano GB, Mortreux G, Beauvillain JC, and Croix D. Evidence for a spontaneous nitric oxide release from the rat median eminence: Influence on gonadotropin-releasing hormone release. *Endocrinology* 142: 2343–2350, 2001.
25. Kosior-Korzecka U and Bobowiec R. Leptin effect on nitric oxide and GnRH-induced FSH secretion from ovine pituitary cells *in vitro*. *J Physiol Pharmacol* 57: 637–647, 2006.
26. Lam TK, Schwartz GJ, and Rossetti L. Hypothalamic sensing of fatty acids. *Nat Neurosci* 8: 579–584, 2005.
27. Marsollier N, Kassis N, Mezghenna K, Soty M, Fioramonti X, Lacombe A, Joly A, Pillot B, Zitoun C, Vilar J, Mithieux G, Gross R, Lajoix AD, Routh V, Magnan C, and Cruciani-Guglielmacci C. Deregulation of hepatic insulin sensitivity induced by central lipid infusion in rats is mediated by nitric oxide. *PLoS One* 4: e6649, 2009.
28. Maury E and Brichard SM. Adipokine dysregulation, adipose tissue inflammation and metabolic syndrome. *Mol Cell Endocrinol* 314: 1–16, 2010.
29. McCann SM, Mastronardi C, de Laurentiis A, and Rettori V. The nitric oxide theory of aging revisited. *Ann NY Acad Sci* 1057: 64–84, 2005.
30. Munzberg H and Myers MG, Jr. Molecular and anatomical determinants of central leptin resistance. *Nat Neurosci* 8: 566–570, 2005.
31. Perrin C, Knauf C, and Burcelin R. Intracerebroventricular infusion of glucose, insulin, and the adenosine monophosphate-activated kinase activator, 5-aminoimidazole-4-carboxamide-1-beta-D-ribofuranoside, controls muscle glycogen synthesis. *Endocrinology* 145: 4025–4033, 2004.
32. Reaux A, De Mota N, Skultetyova I, Lenkei Z, El Messari S, Gallatz K, Corvol P, Palkovits M, and Llorens-Cortes C. Physiological role of a novel neuropeptide, apelin, and its receptor in the rat brain. *J Neurochem* 77: 1085–1096, 2001.
33. Reaux A, Gallatz K, Palkovits M, and Llorens-Cortes C. Distribution of apelin-synthesizing neurons in the adult rat brain. *Neuroscience* 113: 653–662, 2002.
34. Reis WL, Giusti-Paiva A, Ventura RR, Margatho LO, Gomes DA, Elias LL, and Antunes-Rodrigues J. Central nitric oxide blocks vasopressin, oxytocin and atrial natriuretic peptide release and antidiuretic and natriuretic responses induced by central angiotensin II in conscious rats. *Exp Physiol* 92: 903–911, 2007.
35. Rodríguez EM, Blazquez JL, and Guerra M. The design of barriers in the hypothalamus allows the median eminence and the arcuate nucleus to enjoy private milieus: The former opens to the portal blood and the latter to the cerebrospinal fluid. *Peptides* 31: 757–776, 2010.
36. Shankar R, Zhu J, Ladd B, Henry D, Shen H, and Baron A. Central nervous system nitric oxide synthase activity regulates insulin secretion and insulin action. *J Clin Invest* 102: 1403–1412, 1998.
37. Shankar RR, Wu Y, Shen HQ, Zhu JS, and Baron AD. Mice with gene disruption of both endothelial and neuronal nitric oxide synthase exhibit insulin resistance. *Diabetes* 49: 684–687, 2000.
38. Shimazu T. Innervation of the liver and glucoregulation: Roles of the hypothalamus and autonomic nerves. *Nutrition* 12: 65–66, 1996.
39. Shimazu T and Fujimoto T. Regulation of glycogen metabolism in liver by the autonomic nervous system. IV. Neural control of glycogen biosynthesis. *Biochim Biophys Acta* 252: 18–27, 1971.
40. Shimazu T and Fukuda A. Increased activities of glycogenolytic enzymes in liver after splanchnic-nerve stimulation. *Science* 150: 1607–1608, 1965.
41. Shimazu T, Fukuda A, and Ban T. Reciprocal influences of the ventromedial and lateral hypothalamic nuclei on blood glucose level and liver glycogen content. *Nature* 210: 1178–1179, 1966.
42. Soriguer F, Garrido-Sanchez L, Garcia-Serrano S, Garcia-Almeida JM, Garcia-Arnes J, Tinahones FJ, and Garcia-Fuentes E. Apelin levels are increased in morbidly obese subjects with type 2 diabetes mellitus. *Obes Surg* 19: 1574–1580, 2009.
43. Sunter D, Hewson AK, and Dickson SL. Intracerebroventricular injection of apelin-13 reduces food intake in the rat. *Neurosci Lett* 353: 1–4, 2003.
44. Taheri S, Murphy K, Cohen M, Sujkovic E, Kennedy A, Dhillo W, Dakin C, Sajedi A, Ghatei M, and Bloom S. The effects of centrally administered apelin-13 on food intake, water intake and pituitary hormone release in rats. *Biochem Biophys Res Commun* 291: 1208–1212, 2002.
45. Tatemoto K, Takayama K, Zou MX, Kumaki I, Zhang W, Kumano K, and Fujimiya M. The novel peptide apelin lowers blood pressure via a nitric oxide-dependent mechanism. *Regul Pept* 99: 87–92, 2001.
46. Tiraby C, Tavernier G, Capel F, Mairal A, Crampes F, Rami J, Pujol C, Boutin JA, and Langin D. Resistance to high-fat-diet-induced obesity and sexual dimorphism in the metabolic responses of transgenic mice with moderate uncoupling protein 3 overexpression in glycolytic skeletal muscles. *Diabetologia* 50: 2190–2199, 2007.
47. Valle A, Hoggard N, Adams AC, Roca P, and Speakman JR. Chronic central administration of apelin-13 over 10 days increases food intake, body weight, locomotor activity and body temperature in C57BL/6 mice. *J Neuroendocrinol* 20: 79–84, 2008.
48. Yi CX, Serlie MJ, Ackermans MT, Foppen E, Buijs RM, Sauerwein HP, Fliers E, and Kalsbeek A. A major role for perifornical orexin neurons in the control of glucose metabolism in rats. *Diabetes* 58: 1998–2005, 2009.
49. Yue P, Jin H, Aillaud-Manzanera M, Deng AC, Azuma J, Asagami T, Kundu RK, Reaven GM, Quertermous T, and Tsao PS. Apelin is necessary for the maintenance of insulin sensitivity. *Am J Physiol Endocrinol Metab* 298: E59–67, 2010.
50. Zhong JC, Yu XY, Huang Y, Yung LM, Lau CW, and Lin SG. Apelin modulates aortic vascular tone via endothelial nitric oxide synthase phosphorylation pathway in diabetic mice. *Cardiovasc Res* 74: 388–395, 2007.

Address correspondence to:
Dr. Claude Knauf
Université Paul Sabatier
Institut des Maladies Métaboliques et Cardiovasculaires (I2MC)
CHU Rangueil
1 Avenue Jean Poulhes
BP 84225
31432 Toulouse Cedex 4
France

E-mail: claude.knauf@inserm.fr

Date of first submission to ARS Central, July 6, 2010; date of final revised submission, February 25, 2011; date of acceptance, March 13, 2011.

Abbreviations Used

aCSF = artificial cerebrospinal fluid
ARC = arcuate nucleus
DM = dorsomedian hypothalamus
eNOS = endothelial nitric oxide synthase
HD = high dose
HFD = high-fat diet
i.c.v. = intracerebroventricular
ITT = insulin tolerance test
KO = knock-out
LD = low dose
L-NMMA = *N*G-monomethyl-L-arginine
nNOS = neuronal nitric oxide synthase
NO = nitric oxide
NOS = nitric oxide synthase
OGTT = oral glucose tolerance test
SNAP = S-nitroso-*N*-acetyl-D,L-penicillamine
VMH = ventromedian hypothalamus

This article has been cited by:

1. A. Drougard, T. Duparc, A. Gouaze, L. Carneiro, M.X. Brenachot, T. Cadoudal, M.A. Colom, J. Lesage, D. Vieau, A. Benani, C. Leloup, P. Cani, P. Valet, C. Knauf. 2012. Implication de l'apéline hypothalamique dans la mise en place d'un diabète de type 2 par le contrôle de la production hépatique de glucose via le système nerveux autonome. *Annales d'Endocrinologie* **73**:4, 410. [CrossRef]
2. Patrick R. Maloney, Pasha Khan, Michael Hedrick, Palak Gosalia, Monika Milewski, Linda Li, Gregory P. Roth, Eduard Sergienko, Eigo Suyama, Eliot Sugarman, Kevin Nguyen, Alka Mehta, Stefan Vasile, Ying Su, Derek Stonich, Hung Nguyen, Fu-Yue Zeng, Arianna Mangravita Novo, Michael Vicchiarelli, Jena Diwan, Thomas D.Y. Chung, Layton H. Smith, Anthony B. Pinkerton. 2012. Discovery of 4-oxo-6-((pyrimidin-2-ylthio)methyl)-4H-pyran-3-yl 4-nitrobenzoate (ML221) as a functional antagonist of the apelin (APJ) receptor. *Bioorganic & Medicinal Chemistry Letters* . [CrossRef]
3. Isabelle Castan-laurell, Cédric Dray, Claude Knauf, Oxana Kunduzova, Philippe Valet. 2012. Apelin, a promising target for type 2 diabetes treatment?. *Trends in Endocrinology & Metabolism* **23**:5, 234-241. [CrossRef]
4. George R. Pope, Emma M. Roberts, Stephen J. Lolait, Anne-Marie O'Carroll. 2012. Central and peripheral apelin receptor distribution in the mouse: Species differences with rat. *Peptides* **33**:1, 139-148. [CrossRef]
5. Seyyed M. R. Kazemi-Bajestani, Vaibhav B. Patel, Wang Wang, Gavin Y. Oudit. 2012. Targeting the ACE2 and Apelin Pathways Are Novel Therapies for Heart Failure: Opportunities and Challenges. *Cardiology Research and Practice* **2012**, 1-11. [CrossRef]